Multi-Strain Analysis Reveals Distinct Light and Temperature Growth Optima for Morphologically Similar Cyanobacteria

By

Yahya Farooqi

A thesis submitted to the
Department of Biology
Mount Allison University
in partial fulfillment of the requirements for the
Bachelor of Science degree with Honours in Biology
April 11, 2022

Table of Contents

Table of Figures and Tables

Abstract

Picocyanobacteria are small cyanoprokaryotes (0.2-3 μm) that play a large role in global primary production. Given the effects of climate change, picocyanobacterial distribution and localized growth rates may produce overgrowth that can cause negative effects on global biogeochemical cycles and food webs. In this study, we developed a matrix of three light conditions and four ecologically relevant temperature conditions to test the growth rates of six diverse strains of picocyanobacteria in order to predict how picocyanobacteria will grow as global water temperatures increase. Using modified Gompertz models and generalized additive modelling approaches, I uncovered a diverse range of growth optima for both cell count growth rates and chlorophyll growth rates that reveal a general preference for warmer temperatures. Given localized climate trends, we can predict that picocyanobacterial growth rates will increase as much as 40% within the coming century.

Introduction

Picocyanobacteria are a group of cyanoprokaryotes ranging from 0.2-3 μm in diameter (Jasser and Callieri 2016). This group of cyanobacteria are nearly geographically ubiquitous as they are found in both marine and freshwater environments (Scanlan *et al.* 2009) . Furthermore, picocyanobacteria play a large role in global primary production, as they are estimated to constitute roughly 25% of global primary production (Flombaum *et al.* 2013), and contribute nearly 80-90% of carbon production in oligotrophic lakes (Stockner 1988). This group of organisms includes genera *Synechococcus*, *Prochlorococcus*, *Cyanobium*, and *Synechocystis* (Komárek *et al.* 2020) (Lopes *et al.* 2012). Phylogenetic relationships among the *Synechococcus*, *Cyanobium*, and *Synechocystis* genera can be seen in figure 1. *Prochlorococcus* can be found in oligotrophic marine environments (Thompson *et al.* 2018), whereas *Synechococcus* is distributed across marine and freshwater systems (Kim *et al.* 2018). *Cyanobium* is found along similar distributions but has particularly been linked to brackish (Larsson *et al.* 2014) and freshwater systems (Cabello-Yeves *et al.* 2018). *Synechocystis*, in contrast, is found in freshwater systems (Jasser and Callieri 2016).

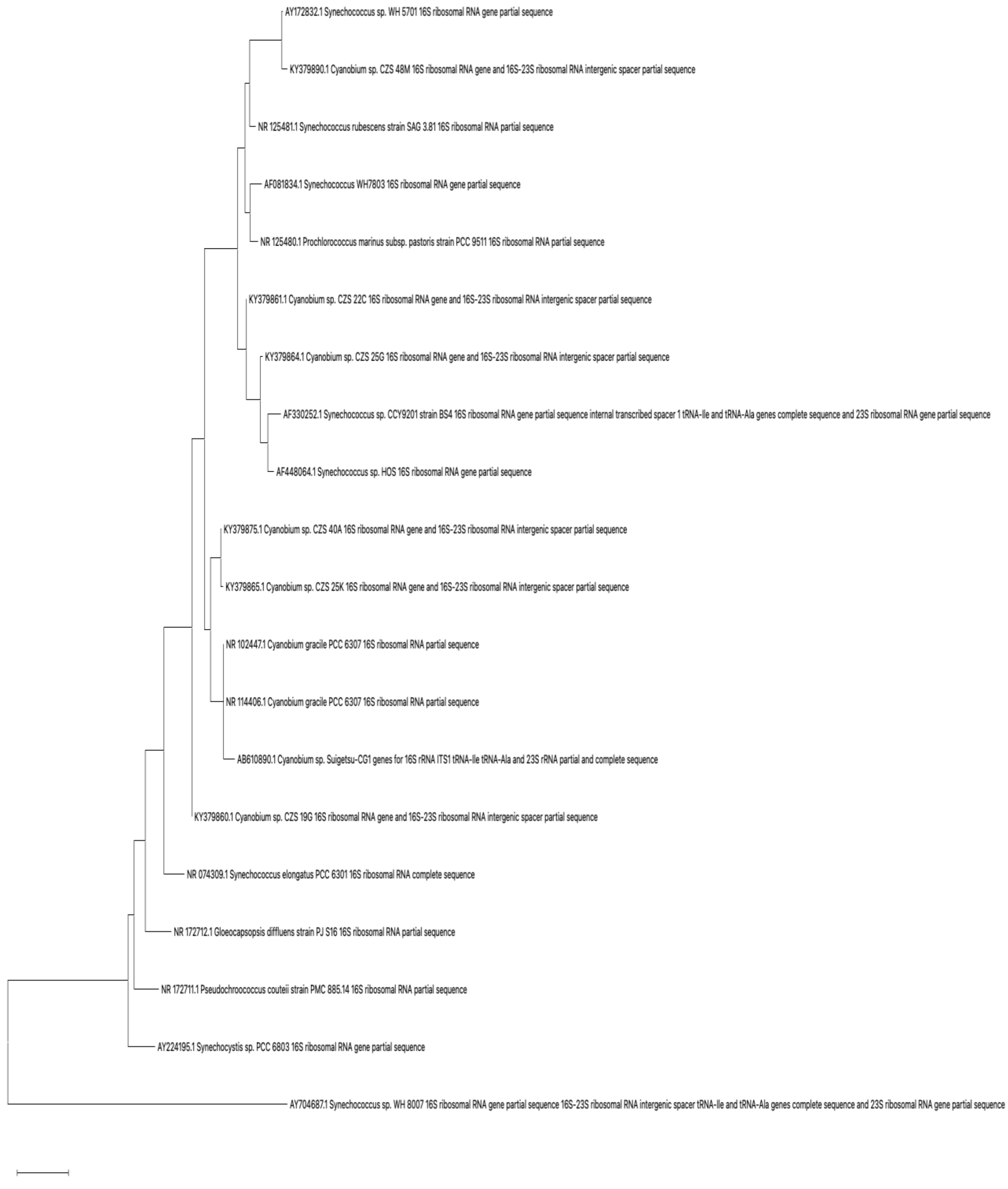

Figure 1: Maximum likelihood phylogenetic tree constructed with MegaX software and 16s ribosomal RNA sequences of a variety of algal strains obtained from NCBI

Recent climate reports suggest that global and oceanic temperatures will continue to increase in response to fossil fuel emissions (Zandalinas, Fritschi, and Mittler 2021). Along with changes in nutrient availability, particularly nitrogen and phosphorus (Berthold and Campbell 2021), increasing temperatures will affect the growth dynamics of picocyanobacterial strains found in marine and freshwater environments as warmer temperatures have been shown to select for smaller organisms both within and among populations across taxa (Zohary, Flaim, and Sommer 2021). This response was first noted by Bergmann in 1847, as he demonstrated that a lower surface area to volume ratio in biological organisms better facilitates thermoregulation (Salewski and Watt 2017). This general trend of smaller sizes being associated with warmer temperatures does not only apply to endotherms but can also be seen to manifest in phytoplankton (Sommer *et al.* 2017). Thus, following Bergmann's general rule, a rise in global temperatures due to climate change may cause a substantial organism size decrease across taxa (Gardner *et al.* 2011). This principle has been substantiated for phytoplankton across three levels: evolutionary evidence, field evidence, and experimental evidence (Zohary, Flaim, and Sommer 2021). Evolutionarily phytoplankton taxa have been shown to decrease in size in response to temperature. Mousing *et al.* (2017) showed that dinoflagellate cyst micro-fossils found in the West Greenland shelf were significantly smaller through time periods with increased temperatures. Phytoplankton size has also been shown to decrease with temperature in field studies, as Winder, Reuter, and Schladow (2009) found that over a 24-year period smaller diatoms came to dominate lake Tahoe, which was correlated to increasing temperatures in the region. Furthermore, a similar study performed by Abonyi *et al.* (2020) showed that phytoplankton cell size decreased over a 34-year period in the river Danube, which was again linked to global climate change. Specific experimental evidence showcasing this effect of decreasing sizes with increasing temperatures was shown by Pulina *et al.* (2016) as phytoplankton sizes decreased in response to warmer temperatures in artificial indoor incubated units. Outdoor mesocosm experiments also show that phytoplankton shift towards smaller sizes in increased temperatures in freshwater conditions (Yvon-Durocher *et al.* 2011). Given these findings, and the fact that smaller marine protists (Atkinson, Ciotti, and Montagnes 2003) and phytoplankton cells (Banse 1976) grow faster with decreasing cell size, I hypothesize that under rising temperature conditions picocyanobacterial strains will increase their growth rates within an environmentally plausible range.

The dominance of small phytoplankton in these conditions must be understood in the context of a variety of factors, including physiological changes and environmental effects, and the interactions therein. Physiologically, phytoplankton responses to increasing temperatures tend to follow the Q10 model, which describes the positive relationship between temperature and metabolic activity over a 10 ℃ range (Mundim *et al.* 2020). This has been postulated to be the result of an increase in kinetic energy within cells due to the increase in temperature (Clarke and Fraser 2004), which as a result increases rates of photosynthesis, respiration, and cell growth, among other processes (Zohary, Flaim, and Sommer 2021). Warming waters also have effects on the stratification of lakes (Boehrer and Schultze 2008) and oceanic water bodies (G. Li *et al.* 2020) which can directly affect phytoplankton populations. Increased temperatures affect water bodies by inducing stratification and by consequence reducing turbulence and mixing which causes the segregation of nutrient availability (Naselli-Flores, Zohary, and Padisák 2021). This decrease in nutrient availability favors the growth of smaller phytoplankton, as having a lower surface area to volume ratio facilitates more efficient nutrient uptake (Van de Waal and Litchman 2020). This difference in surface area to volume ratios can be substantial, as the range of phytoplankton sizes is very broad (Figure 2). Furthermore, the stratification of water bodies benefits smaller phytoplankton due to the principles of Stoke's equation and its interaction with cell sinking rates (Zohary, Flaim, and Sommer 2021). As described by Stoke's equation, low cell sinking rates are dependent on high water viscosity and density, both of which decrease in response to increasing temperatures (Rosas-Navarro, Langer, and Ziveri 2018). Therefore, increasing temperatures are associated with higher sinking velocities for phytoplankton (Zohary *et al.* 2017). Furthermore, according to Stoke's equation, smaller phytoplankton sink slower than larger competitors based on their size, and thus remain higher in the euphotic zone which gives them an advantage in terms of light availability (Sciascia, De Monte, and Provenzale 2013). Furthermore, population loss rate as a result of cell sinking (losing cells due to sinking past the euphotic zone) is amplified through water body stratification for larger cells, meaning picophytoplankton again may have an advantage over larger competitors in warmer temperatures (Zohary, Flaim, and Sommer 2021).

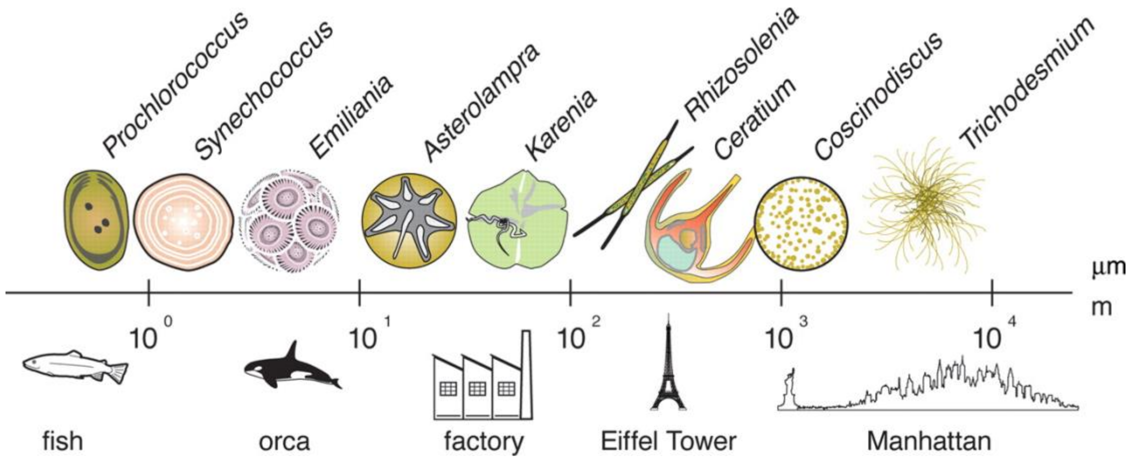

Figure 2: Graphic developed by Finkel *et al.* 2010 outlining the extremely broad difference between the largest and smallest phytoplankton through evolutionary time.

To understand the possible increase in picocyanobacterial growth rates with rising temperatures, the effect of light on cell physiology must also be taken into account. As photosynthetic organisms, picocyanobacteria are dependent on light for energy. This dependence is subject to some variability between and within types of picocyanobacteria (Six *et al.* 2007). Within genera, variability in light dependence can manifest in multiple ways. *Prochlorococcus* ecotypes tend to vary in terms of the levels within the euphotic zone that they inhabit (Bibby *et al.* 2003). *Synechococcus,* in contrast, occupy specialized niche spaces based on differences in pigment content, which provides differential light absorption (Stomp *et al.* 2004). The process of photosynthesis is dependent on highly conserved mechanisms and structures (Mulo, Sicora, and Aro 2009) found across picocyanobacteria genera. In turbulent conditions picocyanobacteria must cope with a range of extreme light conditions, including photoinactivation due to up welling (Six *et al.* 2007). The process of photoinactivation is a result of damage procured by the D1 protein in the PSII structure in high light conditions (Komenda *et al.* 2007). This protein is coded by the *psbA* gene family in picocyanobacteria (Murphy *et al.* 2017), although *Prochlorococcus* only has one form of this gene (Murphy *et al.* 2017; Partensky, Hess, and Vaulot 1999). Within strain variation and between strain variation in regard to photoinactivation responses are notable. Due to this high degree of variability in picocyanobacterial light responses, it is hard to predict how novel strains will grow in different light levels, particularly with varying thermal environments.

As described, the effects of temperature and light have major implications for picocyanobacterial populations. Despite the significance of these factors, it is as yet unknown how the interacting effects of temperature and light levels will influence picophytoplankton growth rates. Establishing these niche spaces is becoming more urgent as the increase in temperature of global water bodies may increase the prevalence of nuisance algal blooms. Such excessive growth, or imbalances of phytoplankton taxa can damage local ecosystems and food-webs (Berthold and Campbell 2021). Analyzing picophytoplankton physiological responses to environmental changes can thus help predict changes in local and global bio-geochemical cycles and food webs as algal overgrowth has been shown to negatively affect both of these environmental parameters (Berthold and Campbell 2021). Furthermore, focusing on responses of only one species/strain will not explain the diversity found in highly dynamic coastal water bodies. In these systems, nutrients, salinity, light, and temperature interactively create a large combination of possible niches. Thus, this study will focus on how light and temperature treatments affect the growth rate and photo-physiological performance of six strains of picophytoplankton with distinct salinity growth optima. I hypothesize that picocyanobacterial growth rates will increase with temperature, with a variable effect of light either independently or interacting with temperature.

Methods

Culturing protocols

Synechococcus sp. CCMP836, *Synechococcus bacillaris* CCMP1333, *Cyanobium* sp. CZS48M, *Cyanobium* sp. NIES981, *Cyanobium* sp. CZS25K, and *Synechocystis* sp. PCC6803 were all grown in BG11 (Stanier *et al.* 1979) derived mineral nutrient media. Strains CCMP836, NIES981, CCMP1333, CZS25K, and CZS48M are all coastal marine/brackish phytoplankton, whereas the strain PCC6803 is primarily freshwater. Artificial sea water (ASW) was prepared following protocols described by Harrison, Waters, and Taylor (1980) and Berges, Franklin, and Harrison (2001). This ASW was used with ultrapure MilliQ to make BG11 derived mineral nutrient media at differing salinities, which represent optimal saline growth environments for the strains used, of 1 ppt (freshwater), 11 ppt, 25 ppt, and 32 ppt (seawater) with nutrient stocks being added after autoclaving. Media was then pH adjusted through titration from 8.0-8.5 to 7.5 with 1 M hydrochloric acid (HCL). Mother cultures were grown on a horizontal shaker by Maximilian Berthold in a 12:12 light:dark diurnal cycle at 22°C and at a light level of 100 µE. Subcultures were performed by Maximilian Berthold every 7 days.

Table 1: BG11 derived mineral nutrient media was composed of the following components and concentrations. Artificial sea water and ultra-pure MilliQ were combined to achieve target salinities, with the resultant solution being autoclaved. Stocks added to media

Component	Stock solution	Quantity per L ddH_20	Molar concentration in final medium
Fe Citrate solution	NA	1 mL	NA
Citric acid	6.0 g L^{-1} dH_2O	------	3.12×10^{-5} M
Ferric ammonium citrate	6.0 g L^{-1} dH_2O	------	3×10^{-5} M
$NaNO_3$	149.6 g L^{-1} dH_2O	10 mL	1.76×10^{-2} M
K_2HPO_4	39.0 g L^{-1} dH_2O	1 mL	2.24×10^{-4} M
$MgSO_4 \bullet 7H_2O$	75.0 g L^{-1} dH_2O	1 mL	3.04×10^{-4} M
$CaCl_2 \bullet 2H_2O$	27.0 g L^{-1} dH_2O	1 mL	1.84×10^{-4} M
Na_2CO_3	20.0 g L^{-1} dH_2O	1 mL	1.89×10^{-4} M
$Na_2EDTA \bullet 2H_2O$*	0.8413 g L^{-1} dH_2O	1 mL	2.26×10^{-6} M
Trace metal solution	See Table 2	1 mL	NA

Table 2: Components used to create trace metal solution used for the creation of BG11 derived mineral nutrient media. These components were filter sterilized by Alyson MacCormack and subsequently stored at 4 °C.

Component	Stock solution	Quantity per L ddH_20	Molar concentration in final medium
H_3BO_3	------	2.860 g	4.63×10^{-5} M
$MnCl_2 \cdot 4H_2O$	------	1.810 g	9.15×10^{-6} M
ZnSO4 $\cdot$ $7H_2O$	------	0.220 g	7.65×10^{-7} M
$CuSO_4 \cdot 5H_2O$	79.0 g L^{-1} ddH_2O	1 ml	3.16×10^{-7} M
$Na_2MoO_4 \cdot 2H_2O$	------	0.391 g	1.61×10^{-6} M
$Co(NO_3)^2 \cdot 6H_2O$	49.4 g L^{-1} ddH_2O	1 ml	1.70×10^{-7} M

Experimental protocol

Well plate preparation

A well plate approach was used for this study. Sterile Falcon non-tissue culture treated 4X6 24 well plates were used to create four technical replicates of each of the six strains tested. Magnetized metal stir bars were sterilized with 70% ethanol and placed into each well after drying. Each of these strains has an optimal salinity, so 2 mL of media of the optimal salinity was added into the corresponding wells using an Opentron Robot Pipettor (Model: OT2, Opentrons, Brooklyn, NY). Plates loaded with media were then read with the ClarioStar micro-plate reader to obtain blank values over wavelength ranges 370-750 nm. Mother cultures were then obtained from Maximilian Berthold, with 0.5 mL of culture being added to each well with absorbance (370-750 nm) and fluorescence (400-750 nm) measurements being taken on the ClarioStar Micro-plate reader following inoculation to measure chlorophyll content proxy values at OD 680-750 nm, otherwise known as deltaOD, which subtracts a turbidity proxy of 750 nm from a chlorophyll proxy of 680 nm to gain a turbidity corrected chlorophyll absorbance value. Furthermore, OD750 nm measurements were also taken to estimate cell count proxies from turbidity measurements.

Culture Measurements

Three prepared plates were placed in a growth chamber set at one temperature with 30, 100 or 300 µE light levels within this chamber (one plate for each light level). We tested 17, 22, 27 and 32℃, separately three times each (apart from 22 ℃) leading to three biological replicates for each light and temperature level, with four technical replicates being present for each strain per light level within each temperature replicate. Every day well plate cultures were re-suspended using magnetized metal stir bars at 100-250 rpm on the V&P Scientific Inc. Magnetic Tumble Stirrer. Following re-suspension absorbance (370-750 nm) measurements were performed on all wells of each plate using a ClarioStar micro-plate reader. To track the growth of the cultures absorbance/optical density (OD) measurements were subtracted from the blank OD values to indicate true culture growth, as the absorbance value of the media would obscure the actual absorbance of the culture. When the cultures had undergone a doubling at a blank corrected optical density at deltaOD a series of physiological measurements were performed (See appendix). Culture from one well plate row per light level was sacrificed to perform cell counts and measure chlorophyll content using established protocols in the lab (Anderson, 2005). Chlorophyll content was analyzed by adding 20 µL of extracted culture in 2 mL of chlorophyll extraction solvent (3:2 Acetone:DMSO) in borosillicate glass cuvettes. The resultant solution was then left in the dark for approximately 25 minutes and subsequently analyzed on a Turner fluorometer (non-acid program) to obtain RFU values. Cell counts were performed by using 50 µL of extracted samples which were diluted in 200 µL of appropriate media in a 96 well plate. The resultant solution was then loaded into a hemocytometer (10 µL) and left for 10 minutes to stabilize cells. ToupView software was used to take pictures using the Leica microscope at 40X magnification. All data gained through these analyses is stored on the Campbell Lab dropbox: (*https://www.dropbox.com/work/Phylis%20Campbell/MURIS/Light_Temp*). The preparation of 3 well plates per temperature condition and light level, and the resultant physiological measurements was repeated a total of 3 times at 17, 27, and 32℃, but only once for 22℃. The missing 22 ℃ data was obtained and incorporated into my dataset from previous experiments run by Maximillian Berthold, however this supplementary data did not include data for PCC6803.

Data analysis

The data obtained from this study was analyzed using RStudio (RStudio Team, 2021). Existing R notebooks developed by Maximilian Berthold and Douglas A. Campbell were used and adapted by me for the data gained in this study. Data pipelines and manipulations were made with the tools provided by the R TidyVerse (Wickham *et al.* 2019). The script repository used in this study is available on GitHub: (*https://github.com/GitHubDoug/FundyPhytoPhysCodeChunks*).

Data import

Scripts developed by Maximilian Berthold and Douglas A. Campbell were used to import and analyze the deltaOD and OD 750 nm data obtained from the ClarioStar micro-plate reader. Scripts developed by the same authors were used to import chlorophyll content RFU data.

Regression fit

Strains with larger cell sizes may report the same absorbance values relative to smaller strains despite having fewer total cells present in culture. To correct this disparity in absorbance reporting and to establish a strain specific and light specific relationship between cell counts and absorbance cell count proxy measurements a regression was performed between measured cell counts and OD750 nm absorbance readings, which is a proxy for cell count / turbidity (See appendix). The resultant slope was used to interpolate cell count estimates for OD750 nm readings across strains and light levels. Similarly, reporting of cell chlorophyll content using deltaOD may be inaccurate as chlorophyll content relative to cell size may differ between strains and light levels. To help establish the strain specific and light specific relationship between chlorophyll content and deltaOD a regression was constructed between chlorophyll extraction data and deltaOD absorbance values (See appendix). These regressions allowed us to calculate cell counts (cells/mL^{-1}) chlorophyll content (µg L^{-1}) based on our absorbance measurements.

Data fitting

Growth rates of the regression corrected deltaOD data gained across light levels, temperatures, and strains were extracted to fit modified Gompertz (Zwietering *et al.* 1992) and Logistic (Peleg and Corradini 2011) growth models using scripts developed by Douglas A. Campbell and Maximilian Berthold. R scripts employed the use of "nlsMicrobio," (Baty *et al*. 2014) "nlstools," (Baty *et al*. 2015) and "minpack.lm" (Elzhov *et al*. 2016) packages to fit the data to the relevant models. The logistic model equation (Equation 1) employed both our corrected optical density measurements (regression corrected deltaOD and OD 750 nm) as representative of population ($N(t)$) as a function of time.

Equation 1:

$$N(t) = \frac{N_{asymp} N_o exp(\mu t)}{[N_{asymp} + (N_o exp(\mu t) - 1)]}$$

Variable N_{asymp} represents the population number reaching stationary phase (maximum). μ represents the specific exponential growth rate and N_o represents the initial size of the population. A modified Gompertz equation (Equation 2) was also employed to fit culture growth.

Equation 2:

$$log(\frac{N(t)}{N_{min}}) = Aexp[-exp[\frac{\mu_m exp(1)}{A}(\lambda - t) + 1]]$$

As previously defined, $N(t)$ is the population as a function of time. The N_{min} term is the minimum size achieved by the population, the A term is the asymptote towards the maximal population value achieved, μ_m is the maximum specific growth rate, and λ is the lag time.

Statistical Analysis

ART ANOVA Approach

The aligned rank transform ANOVA was employed in this study to establish light and temperature effects on each strain individually. Light and temperature were taken to be the independent variables and modified Gompertz growth rate estimates were taken to be the dependent variable. The null hypothesis was that no significant difference in means would be detected across light levels or temperature levels, and that there will be no interaction between factors. Both chlorophyll (deltaOD) and cell count (OD 750 nm) growth rates were tested individually per strain, resulting in two ART ANOVA's being performed for all six strains tested. Post-hoc testing to establish factor level differences was conducted using the "art.con" function from the "ARTool" package. If an interaction term was significant, the data were split by light level, and a Kruskal-Wallace test was performed to establish the effect of temperature per light level.

PERMANOVA Approach

A PERMANOVA approach was used to establish the effect of temperature and light across the six strains of picocyanobacteria in regard to their modified Gompertz growth rate estimates. Light and temperature were treated as the independent variables and the six strains as the dependent variables. The null hypothesis for this test was that no significant difference will be found across light levels, that no significant difference will be found in means between temperature levels, and that there will be no significant interaction between light and temperature. This test was performed on both the cell count growth rate data, and the chlorophyll growth rate data. Post-hoc testing was done using the "pairwise.adonis" function from the "vegan" package (Oksanen *et al.* 2013). Furthermore, bray-curtis distances were calculated to test for the significance of dispersion to ensure PERMANOVA results are interpretable, and to create NMDS plots of both light and temperature groups for both cell count and chlorophyll growth rate data. If dispersion was significant, an NMDS plot was consulted to check for centroid clustering.

Generalized Additive Modelling

Generalized additive modelling was used to characterize strain specific growth optima across light (30-300 μE) and temperature conditions (17-32 °C). This quadratically penalized likelihood approach was conducted with the following formula:

μ ~ s(PAR, k = 3) + s(Temperature (C), k = 4) + ti(Temperature (C), PAR, k = 3).

Smoothing terms (s) for growth rate estimates were light and temperature, with the knot parameter (k) being set to three for light and four in regard to temperature. A tensor product (ti) to account for light and temperature interaction was also added with the knot parameter being set to 3. Furthermore, each model value greater than a 10% standard error was filtered out of this analysis. This approach was used to model growth of each strain for both cell count growth rate data and chlorophyll growth rate data. Visualizations of general growth rate trends across matrix conditions were performed alongside growth optima visualization which represent only the top 10 % of growth rates.

Biovolume measurement

Biovolume was calculated through measuring the length and width of cell count pictures using the ImageJ software. Ten measurements were made for each interacting light and temperature level which were then plotted to visualize biovolume trends across light and temperature conditions.

Results

Strain Specific Growth Preference Assessment

PCC6803

An aligned rank transformed ANOVA (ART ANOVA) was performed on cell count growth rate data (figure 3A) and chlorophyll growth rate data (figure 3B) for PCC6803. Due to missing replicates for the 22 °C temperature level, this analysis was performed only considering the 17, 27, and 32 °C temperature levels. Generalized additive modelling (GAM) was also performed to visualize preferred growth spaces for this strain within a matrix of light and temperature conditions based on cell count growth rate estimates (Figure 3C) and growth rate estimates derived from relative increases in chlorophyll content (figure 3D).

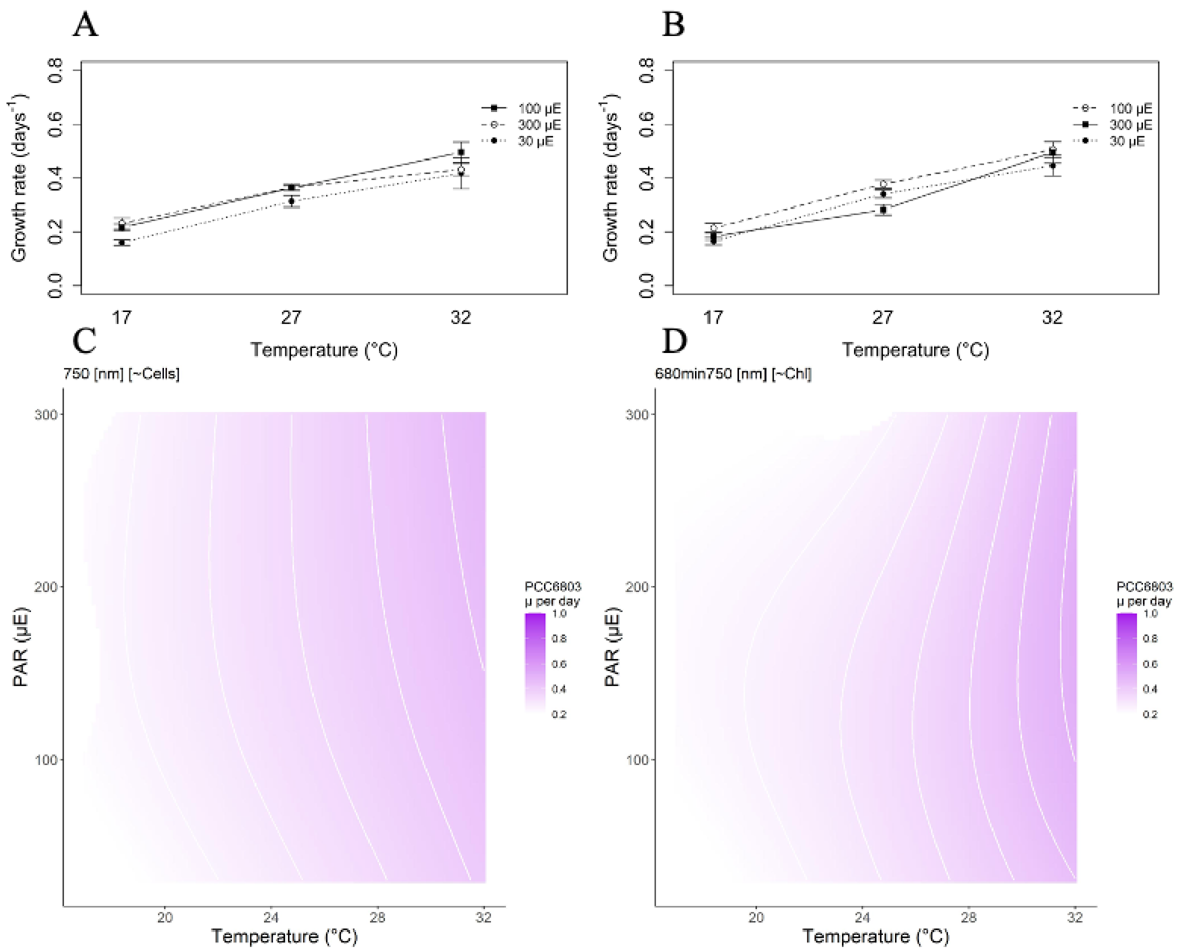

Figure 3: Modified Gompertz growth rate estimates of PCC6803 within combinations of light and temperature conditions, and GAM visualizations showing preferred growth environments. A: Modified Gompertz growth rate estimates are derived from cell count increases over a range of three light and temperature conditions, as derived from the slope equation of a regression of OD750 nm absorbance culture growth data against cell counts. **B**: Modified Gompertz growth rate estimates derived from chlorophyll increases over a range of three light and temperature conditions, as derived from the slope equation of a regression of OD680-750 nm (deltaOD) absorbance culture growth data against chlorophyll extraction data. **C**: Predicted growth rates provided by a generalized additive model based on PCC6803 cell count growth rates over four temperature conditions and three light levels. **D**: Predicted growth rates provided by a generalized additive model based on PCC6803 chlorophyll content growth rates over four temperature conditions and three light levels. Generalized additive models used light and temperature as smoothing functions.

The ART ANOVA analysis performed on the cell count growth rate estimates found temperature to be highly significant ($F_{df=2}$ =79.29, p<0.0001) and light to be significant ($F_{df=2}$ =5.55, p=0.0069), with no significant interaction term ($F_{df=4}$ =0.85, p=0.50). A post-hoc analysis was conducted using the “art.con” function which found significant differences between all temperature levels ($p<0.05$) and significant differences between the 30-300 μE light levels ($p<0.05$).

The ART ANOVA analysis on chlorophyll growth rate data detected a highly significant difference in temperature level means ($F_{df=2}$ =183.61, $p<0.0001$) and a significant effect of light ($F_{df=2}$ =4.15, p=0.022), with no significant interaction term ($F_{df=4}$ =0.90, p=0.47). A post-hoc analysis was conducted using the “art.con” function which found significant differences between all temperature levels ($p<0.05$) and significant differences between the 30 and 100 μE light levels and the 100 and 300 μE light levels ($p<0.05$).

A generalized additive model based on cell count growth rate data found that PCC6803 cell growth preference is found at high temperatures and a broad range of light levels, with a slight preference for higher light levels (figure 3C), which corresponds to our statistical testing. Models based on chlorophyll increases (Figure 3D) found that the highest increases in chlorophyll content occur at higher temperatures, generally at medium light levels ranging from 50 to 200 μE, which also corresponds to our statistical tests.

CZS25K

The same ART ANOVA analysis was performed on cell count growth rate data (figure 4A) and chlorophyll growth rate data (figure 4B) for CZS25K. Generalized additive modelling (GAM) was also performed to visualize preferred growth spaces for this strain within a matrix of light and temperature conditions based on cell count growth rate estimates (figure 4C) and growth rate estimates derived from relative increases in chlorophyll content (figure 4D).

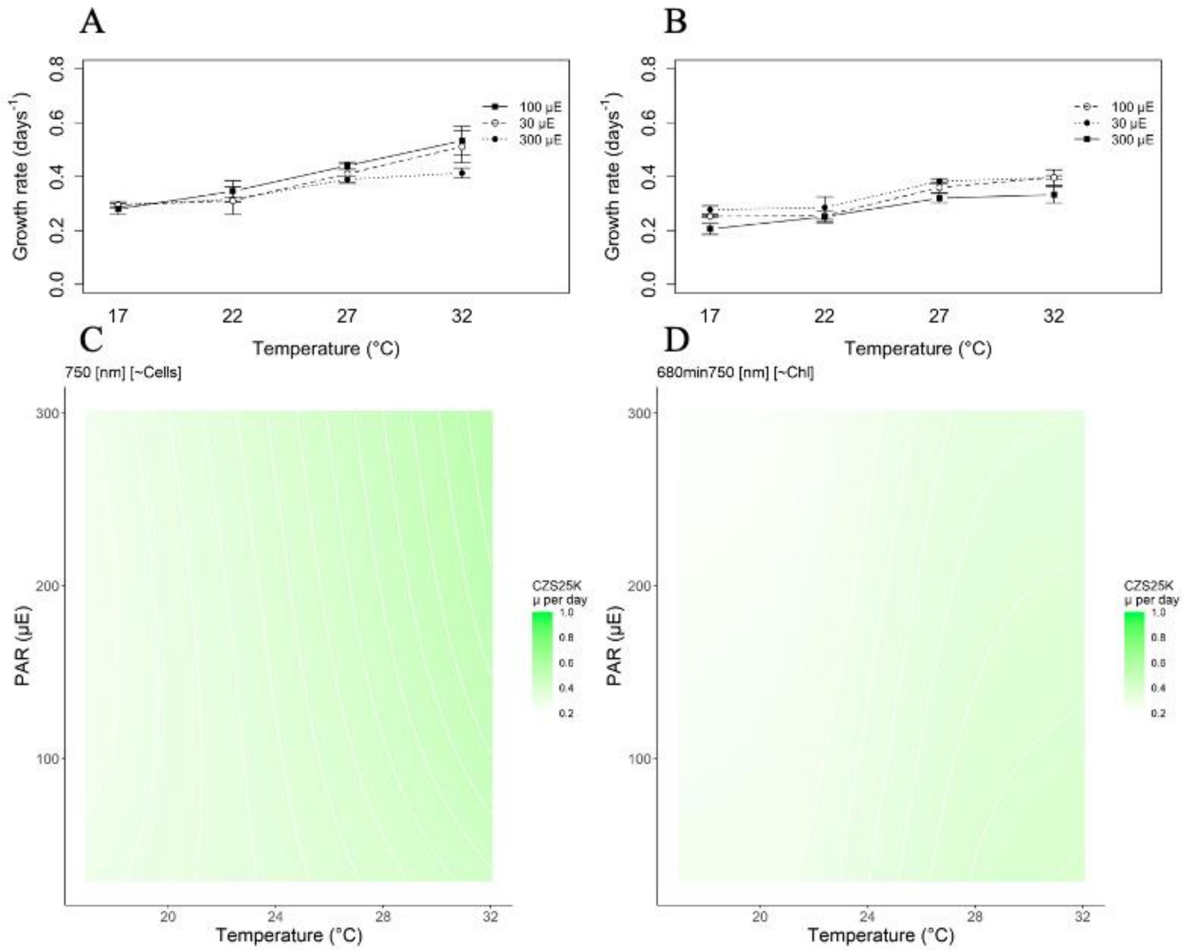

Figure 4: Modified Gompertz growth rate estimates of CZS25K within combinations of light and temperature conditions, and GAM visualizations showing preferred growth environments. A: Modified Gompertz growth rate estimates are derived from cell count increases over a range of three light conditions and four temperature conditions, as derived from the slope equation of a regression of OD750 nm absorbance culture growth data against cell counts. **B**: Modified Gompertz growth rate estimates derived from chlorophyll increases over a range of three light and four temperature conditions, as derived from the slope equation of a regression of OD680-750 nm (deltaOD) absorbance culture growth data against chlorophyll extraction data. **C**: Predicted growth rates provided by a generalized additive model based on CZS25K cell count growth rates over four temperature conditions and three light levels. **D**: Predicted growth rates provided by a generalized additive model based on CZS25K chlorophyll content growth rates over four temperature conditions and three light levels. Generalized additive models used light and temperature as smoothing functions.

The ART ANOVA analysis performed on the cell count growth rate estimates found temperature to be highly significant ($F_{df=3} = 36.67$, $p<0.0001$) and light to be non-significant ($F_{df=2} = 2.87$, $p=0.066$), with no significant interaction term ($F_{df=6} = 1.04$, $p=0.41$). A post-hoc analysis was conducted using the "art.con" function which found significant differences between all temperature levels ($p<0.05$) apart from the 17-22 °C and 27-32 °C levels.

The result of the ART ANOVA on chlorophyll growth rate estimates indicated a significant difference across temperature levels ($F_{df=3}=35.49$, $p<0.0001$) and light levels ($F_{df=2}=7.11$, $p=0.0019$), with no significant interaction effect being found ($F_{df=6}=0.33$, $p=0.92$). A post-hoc comparison was conducted to establish factor level differences using the "art.con" function which indicated significant differences in all temperature levels ($p<0.05$) except for the 17-22 °C and 27-32 °C level comparisons. Furthermore, only the 30-300 µE and 100-300 µE light level comparisons were significant ($p<0.05$).

A generalized additive model based on cell count growth rates found that CZS25K cell growth preference is found at high temperatures and high light levels (figure 4C). This temperature preference is supported by the statistical tests performed; however, the light preference was not found to be significant. Models based on chlorophyll growth rates (Figure 4D) found that the highest increases in chlorophyll content occur at higher temperatures, and at lower light levels, with both results being confirmed by the ART ANOVA results.

CCMP1333

An ART ANOVA analysis was done on cell count growth rate data (figure 5A) and chlorophyll growth rate data (figure 5B) for CCMP1333. Generalized additive modelling (GAM) was also performed to visualize preferred growth spaces for this strain within a matrix of light and temperature conditions based on cell count growth rate estimates (figure 5C) and chlorophyll growth rates (figure 5D).

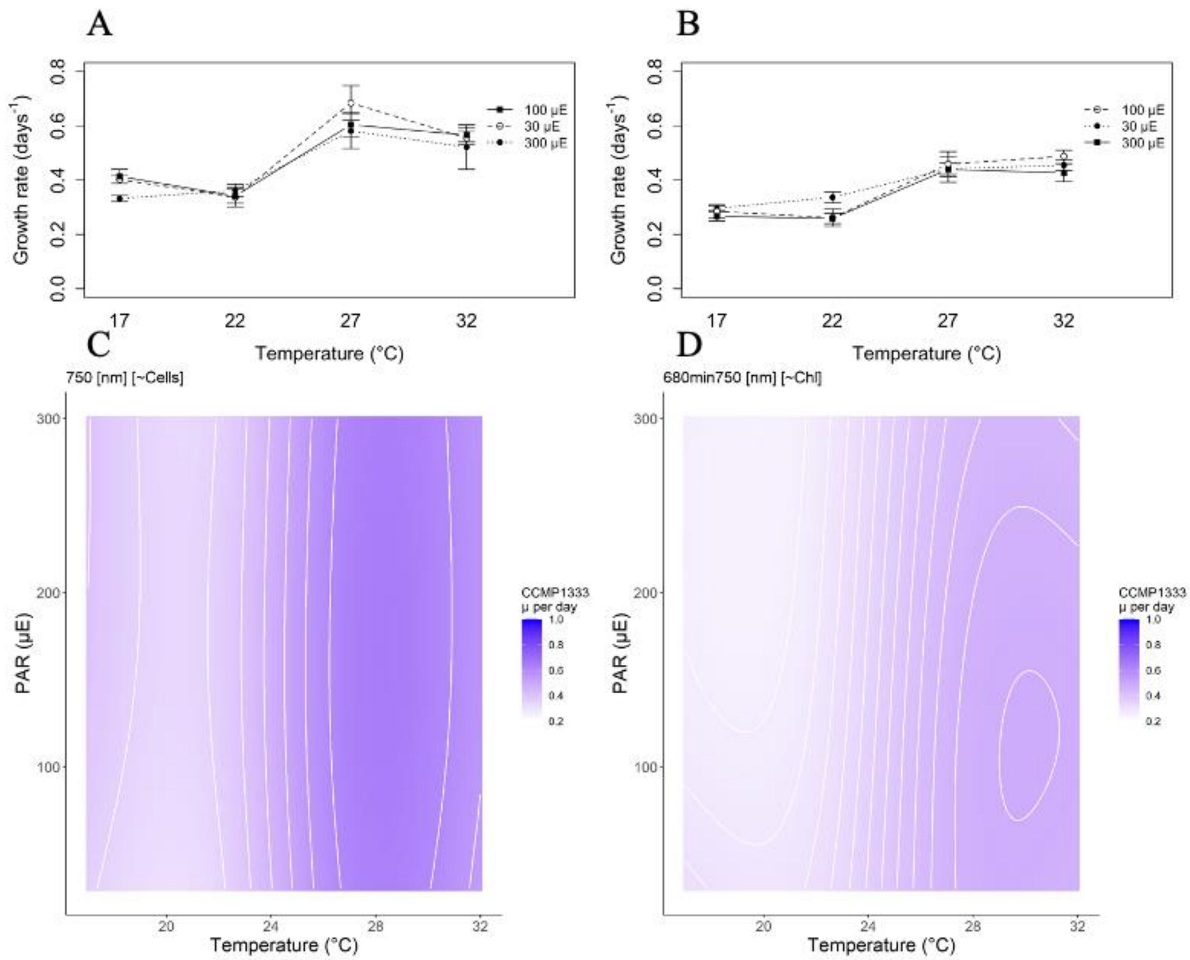

Figure 5: Modified Gompertz growth rate estimates of CCMP1333 within combinations of light and temperature conditions, and GAM visualizations showing preferred growth environments. **A**: Modified Gompertz growth rate estimates are derived from cell count increases over a range of three light conditions and four temperature conditions, as provided by the slope equation of a regression of OD750 nm absorbance culture growth data against cell counts. **B**: Modified Gompertz growth rate estimates derived from chlorophyll increases over a range of three light and four temperature conditions, as provided by the slope equation of a regression of OD680-750 nm (deltaOD) absorbance culture growth data against chlorophyll extraction data. **C**: Predicted growth rates provided by a generalized additive model based on CCMP1333 cell count growth rates over four temperature conditions and three light levels. **D**: Predicted growth rates provided by a generalized additive model based on CCMP1333 chlorophyll content growth rates over four temperature conditions and three light levels. Generalized additive models used light and temperature as smoothing functions

The ART ANOVA analysis performed on the cell count growth rate estimates found temperature to be highly significant ($F_{df=3}=30.75$, $p<0.0001$) with no significant effect of light ($F_{df=2}=1.57$, $p=0.22$), and no significant interaction term ($F_{df=6}=0.58$, $p=0.74$). A post-hoc analysis was conducted using the “art.con” function which found significant differences between all temperature levels ($p<0.05$) apart from the 17-22 °C and 27-32 °C levels.

The chlorophyll growth rate estimate ART ANOVA analysis displayed a highly significant effect of temperature ($F_{df=3}=34.34$, $p<0.0001$) and no significant effect for light levels ($F_{df=2}=0.68$, $p=0.51$) and no interaction ($F_{df=6}=0.73$, $p=0.62$). A post-hoc comparison was conducted to establish temperature level differences using the “art.con” function which indicated significant differences in all temperature levels ($p<0.05$) except for the 17-22 °C and 27-32 °C level comparisons.

A generalized additive model based on cell count growth rates found that CCMP1333 cell growth preference is found at high temperatures (particularly 27-30 °C) across all light levels (figure 5C), which reflects our statistical analysis. Models based on chlorophyll growth rates (Figure 5D) found that the highest increases in chlorophyll content occur at higher temperatures, and at lower light levels, particularly around 100 μE. This temperature preference is reflected in our statistical tests, but the light preference is not.

NIES981

The same ART ANOVA analysis was performed on cell count growth rate data (figure 6A) and chlorophyll growth rate data (figure 6B) for NIES981. Generalized additive modelling (GAM) was also performed to visualize preferred growth spaces for this strain within a matrix of light and temperature conditions based on cell count growth rate estimates (figure 6C) and chlorophyll growth rates (figure 6D)

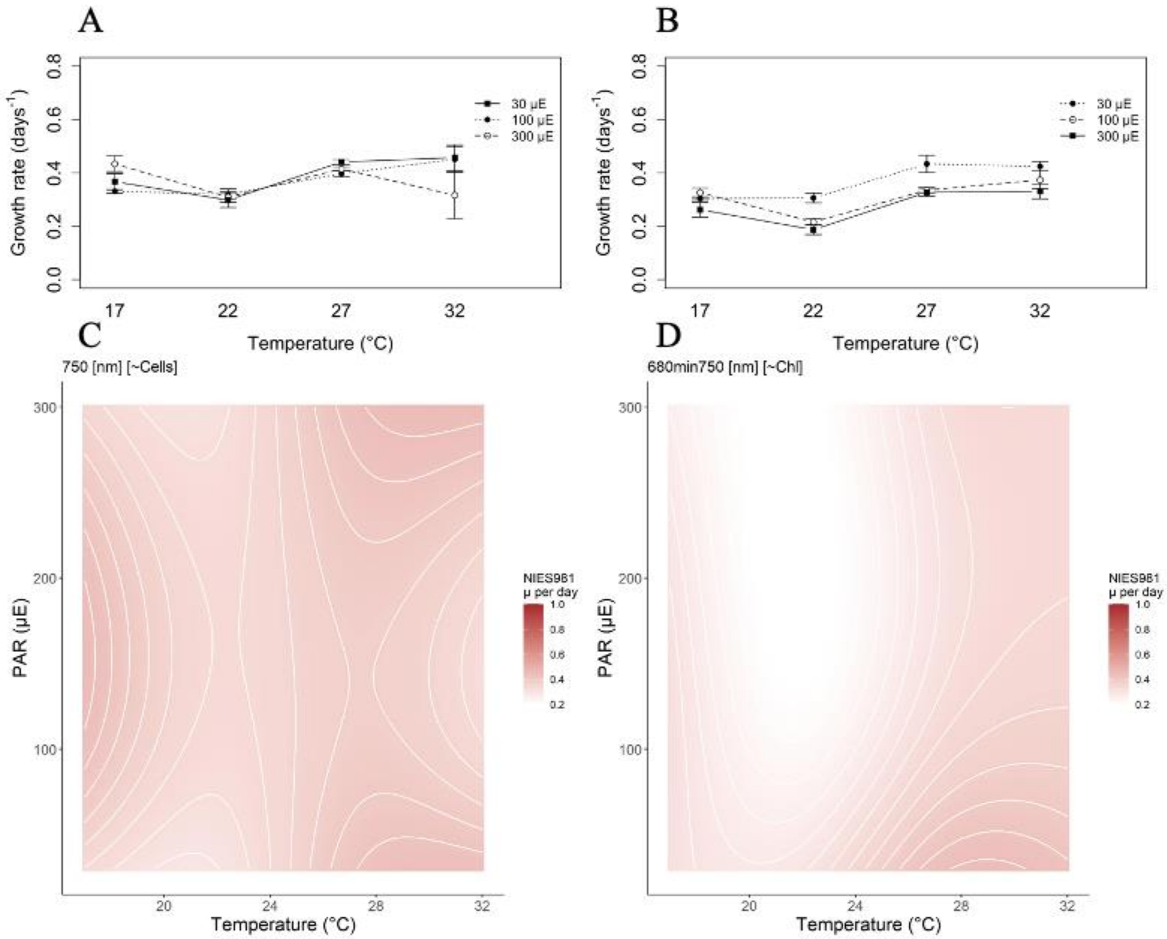

Figure 6: Modified Gompertz growth rate estimates of NIES981 within combinations of light and temperature conditions, and GAM visualizations showing preferred growth environments. A: Modified Gompertz growth rate estimates are derived from cell count increases over a range of three light conditions and four temperature conditions, as provided by the slope equation of a regression of OD750 nm absorbance culture growth data against cell counts. **B**: Modified Gompertz growth rate estimates derived from chlorophyll increases over a range of three light and four temperature conditions, as provided by the slope equation of a regression of OD680-750 nm (deltaOD) absorbance culture growth data against chlorophyll extraction data. **C**: Predicted growth rates provided by a generalized additive model based on NIES981 cell count growth rates over four temperature conditions and three light levels. **D**: Predicted growth rates provided by a generalized additive model based on NIES981 chlorophyll content growth rates over four temperature conditions and three light levels. Generalized additive models used light and temperature as smoothing functions

The ART ANOVA analysis performed on the cell count growth rate estimates found temperature to be highly significant ($F_{df=3}$ =7.24, p=0.00039), with light being non-significant ($F_{df=2}$ =0.65, p=0.53), with no significance for the interaction term ($F_{df=6}$ =2.20, p=0.058). A post-hoc analysis was conducted using the “art.con” function which found significant differences between the 17-22 °C, 22-27 °C, and 22-32 °C temperature levels ($p<0.05$).

The chlorophyll growth rate estimate ART ANOVA analysis showed a significant difference between temperature level means ($F_{df=3} = 20.49$, $p<0.0001$) and light levels means ($F_{df=2} = 13.69$, $p<0.0001$), with no significant interaction term ($F_{df=6} = 1.71$, $p=0.14$). A post-hoc analysis was conducted using the “art.con” function which found significant differences between all temperature levels ($p<0.05$) apart from the 27-32 °C comparison ($p>0.05$) and significant differences between all light levels ($p<0.05$).

A generalized additive model based on cell count growth rates found that NIES981 cell growth optima is found at high temperatures and high (300 µE) and low (30 µE) light levels. Furthermore, high growth rates were also found at low temperatures between 100 and 200 µE (figure 6C). Models based on chlorophyll growth rates (Figure 6D) found that the highest increases in chlorophyll content occur at high temperatures, and at lower light levels, particularly around 30 to 100 µE. The statistical tests performed reflect both the cell count growth rate and chlorophyll growth rate preferences, however it is important to note that the growth response for this strain is slightly unusual due to its preference for high and low temperatures, and aversion to average temperatures.

CCMP836

An ART ANOVA was performed on cell count growth rate data (figure 7A) and chlorophyll growth rate data (figure 7B) for CCMP836. Generalized additive modelling (GAM) was also performed to visualize preferred growth spaces for this strain within a matrix of light and temperature conditions based on cell count growth rate estimates (figure 7C) and growth rates (figure 7D).

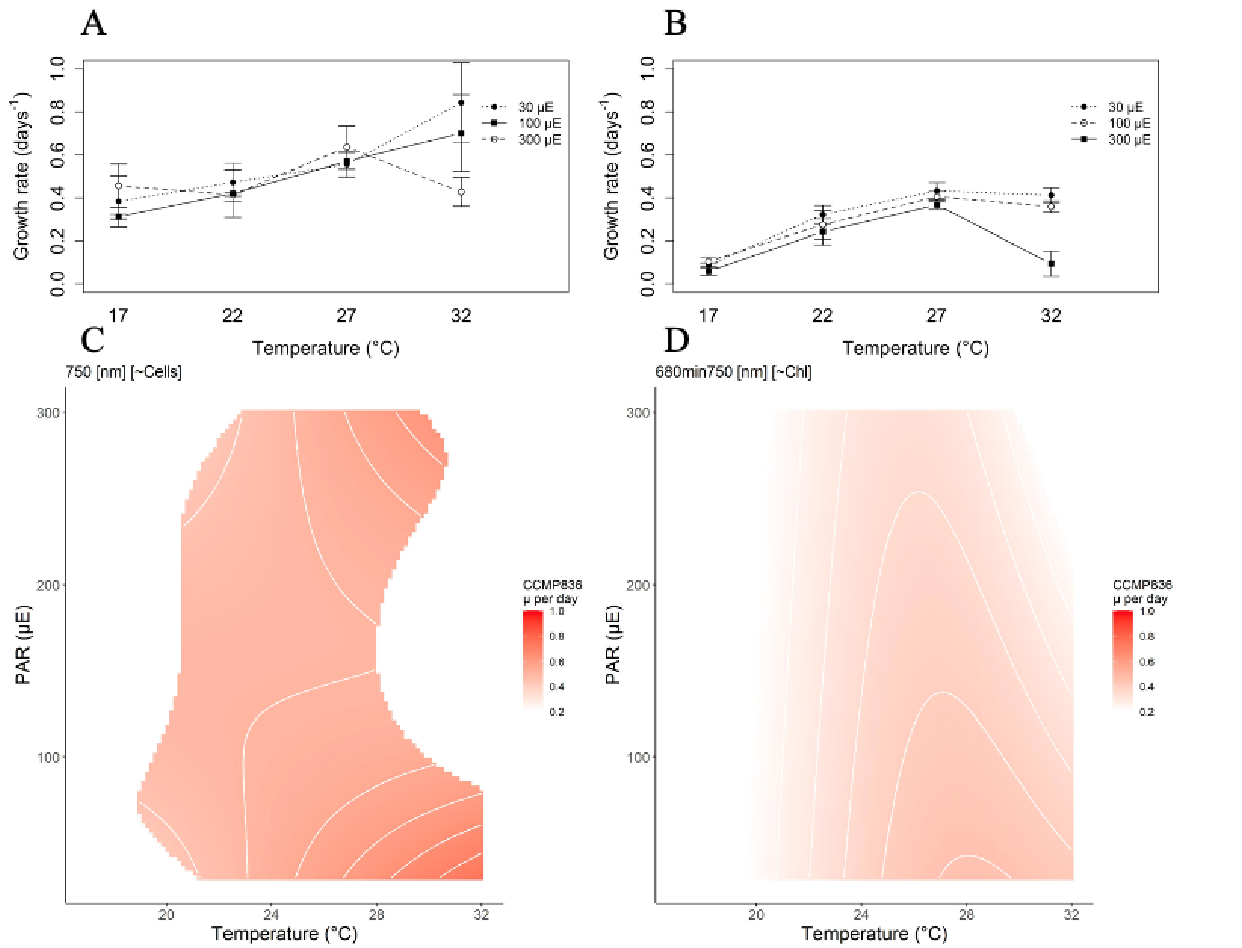

Figure 7: Modified Gompertz growth rate estimates of CCMP836 within combinations of light and temperature conditions, and GAM visualizations showing preferred growth environments. A: Modified Gompertz growth rate estimates are derived from cell count increases over a range of three light conditions and four temperature conditions, as provided by the slope equation of a regression of OD750 nm absorbance culture growth data against cell counts. **B**: Modified Gompertz growth rate estimates derived from chlorophyll increases over a range of three light and four temperature conditions, as provided by the slope equation of a regression of OD680-750 nm (deltaOD) absorbance culture growth data against chlorophyll extraction data. **C**: Predicted growth rates provided by a generalized additive model based on CCMP836 cell count growth rates over four temperature conditions and three light levels. **D**: Predicted growth rates provided by a generalized additive model based on CCMP836 chlorophyll content growth rates over four temperature conditions and three light levels. Generalized additive models used light and temperature as smoothing functions.

The ART ANOVA analysis performed on the cell count growth rate estimates found temperature to be significant ($F_{df=3} = 4.88$, $p=0.0046$) and light to be non-significant ($F_{df=2} = 2.87$, $p=0.066$), with no significance for the interaction term ($F_{df=6} = 1.04$, $p=0.41$). A post-hoc analysis was conducted using the "art.con" function which found significant differences between the 17-27 °C and 17-32 °C temperature levels ($p<0.05$).

For the ART ANOVA performed on the chlorophyll growth rate estimates both light and temperature were found to be significant in this analysis, however the main effects could not be interpreted due to a significant interaction term ($F_{df=6}=3.39$, $p=0.0069$). To understand the effect of temperature, we split our data set by light level and conducted three Kruskal-Wallis tests to test for differences between temperature levels. For the 30 µE light level a significant effect was found for temperature ($p=0.0020$). Post-hoc testing was conducted using the "pairwise.wilcox.test" function from the "stats" R package, which showed significant differences between the 17-27 °C and 17-32 °C levels. The 100 µE light level showed a significant effect of temperature ($p=0.0025$), with post-hoc testing again revealing significant differences between the 17-27 °C and 17-32 °C groups. The 300 µE light level also revealed a significant effect of temperature ($p=0.0035$), with post-hoc testing revealing significant differences between 17-27 °C and 27-32 °C levels.

A generalized additive model based on cell count growth rates found that CCMP836 cell growth preference is found at high temperatures and low light levels (figure 7C), with both of these preferences not clearly being reflected in the statistical analysis above. Models based on chlorophyll growth rates (Figure 7D) found that the highest increases in chlorophyll content occur at high temperatures (27-30 °C), and at lower light levels, particularly around 30 to 100 µE. Due to the interaction, only the temperature preference could be assessed statistically, with the result of this assessment supporting the GAM visualization as it suggests a preference for 27 °C.

CZS48M

An ART ANOVA was performed on cell count growth rate data (figure 8A) and chlorophyll growth rate data (figure 8B) for CZS48M. Generalized additive modelling (GAM) was also performed to visualize preferred growth spaces for this strain within a matrix of light and temperature conditions based on cell count growth rate estimates (figure 7C) and chlorophyll growth rate estimates (figure 7D).

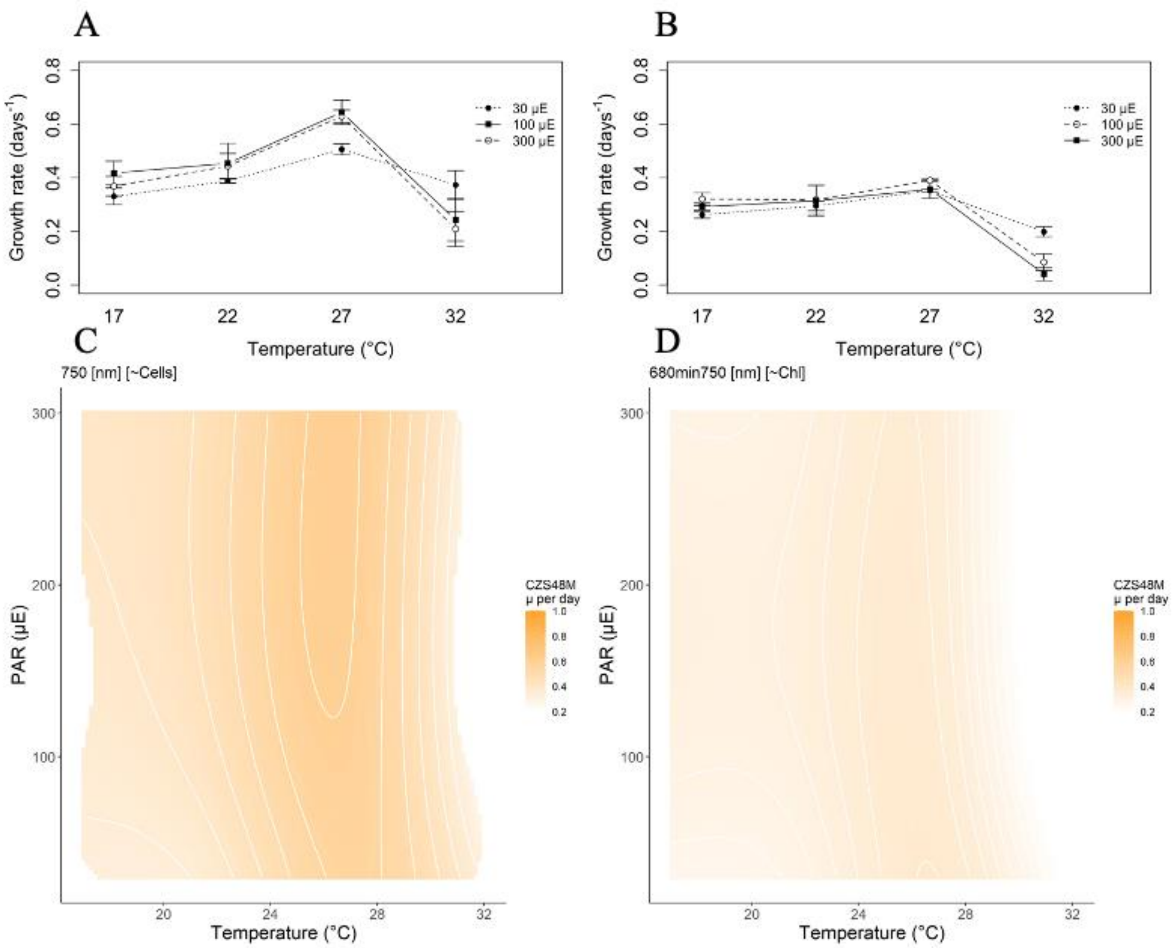

Figure 8: Modified Gompertz growth rate estimates of CZS48M within combinations of light and temperature conditions, and GAM visualizations showing preferred growth environments. A: Modified Gompertz growth rate estimates are derived from cell count increases over a range of three light conditions and four temperature conditions, as provided by the slope equation of a regression of OD750 nm absorbance culture growth data against cell counts. **B**: Modified Gompertz growth rate estimates derived from chlorophyll increases over a range of 3 light and four temperature conditions, as provided by the slope equation of a regression of OD680-750 nm (deltaOD) absorbance culture growth data against chlorophyll extraction data. **C**: Predicted growth rates provided by a generalized additive model based on CZS48M cell count growth rates over four temperature conditions and three light levels. **D**: Predicted growth rates provided by a generalized additive model based on CZS48M chlorophyll content growth rates over four temperature conditions and three light levels. Generalized additive models used light and temperature as smoothing functions.

The ART ANOVA analysis performed on the cell count growth rate estimates found temperature to be highly significant ($F_{df=3}$ =31.19, $p<0.0001$), with no significance being found for light ($F_{df=2}$ =0.29, p=0.74) or the interaction term ($F_{df=6}$ =1.65, p=0.15). A post-hoc analysis was conducted using the "art.con" function which found significant differences between the 17-27 °C, 22-27 °C, 22-32 °C, and 27-32 °C temperature levels ($p<0.05$).

For the chlorophyll growth rate estimate ART ANOVA, the main effects for this analysis could not be interpreted because the interaction term was significant ($F_{df=6}=4.32$, $p=0.0013$). To understand the effect of temperature, we then split our data set by light level and conducted three Kruskal-Wallis tests to test for differences between temperature levels. for the 30 µE light level a significant effect was found for temperature ($p=0.00081$). Post hoc testing was conducted using the "pairwise.wilcox.test" function from the "stats" R package, which showed significant differences between all temperature levels apart from the 17-22 °C comparison. The 100 µE light level showed a significant effect of temperature ($p=0.0023$), with post-hoc testing revealing significant differences between the 17-32 °C and 27-32 °C groups. The 300 µE light level also revealed a significant effect of temperature ($p=0.0041$), with post-hoc testing revealing significant differences between 17-32 °C and 27-32 °C levels.

A generalized additive model based on cell count growth rates found that CZS48M cell growth preference is found at temperatures ranging from 25-28 °C and at all light levels, with a slight preference for light level between 150 and 300 µE (figure 8C). This temperature preference is reflected in the statistical analysis above; however, the light preference is not statistically significant. Models based on chlorophyll growth rates (Figure 8D) found that the highest increases in chlorophyll content again occur at temperatures ranging from 25 to 28 °C, with a slight preference for lower light levels. Due to the interaction, only the temperature preference could be assessed statistically, with the result of this assessment confirming the GAM visualization.

PERMANOVA Approach and Picocyanobacterial Growth Optima Visualization

PERMANOVA

In order to assess the general trend of picocyanobacterial growth responses to varying environmental conditions a two-way PERMANOVA analysis was performed on both cell count growth rate estimates and chlorophyll growth rate estimates. Due to a lack of replicates for the 22 °C temperature level, PCC6803 was excluded from these analyses. Cell count growth rates and chlorophyll growth rates in each strain were taken to be the dependent variables and light and temperature were the independent variables for both of these analyses. The chlorophyll growth rate estimate analysis found no significant interaction between light and temperature (p= 0.26) and a significant effect of light ($F_{df=2}$ =3.02, p=0.023) and of temperature ($F_{df=3}$ =18.9897, p=0.0001). A multivariate homogeneity of variance test was run using the "betadisper" function from the "vegan" package to assess whether the significant PERMANOVA results were due to high variation in dispersion for both light and temperature levels. This analysis yielded a non-significant p-value for both light (p=0.065) and temperature (p=0.12) which indicates the PERMANOVA results are interpretable. Post-hoc testing was performed using the "pairwiseAdonis" package which found significant differences between all temperature groups and no significant differences between light levels. This finding of no significance for light levels in post-hoc testing, along with a marginal dispersion test p-value (p=0.065) and high clustering in the NMDS visualization (Figure 9B), indicate that light is probably statistically significant, but not biologically significant. Indicator values were also calculated using the "IndVal" function to represent strain fidelity and relative abundance among the environmental variables tested. Temperature indicator values were tested for significance using the "multiplatt" package and found significant associations between CCMP1333 (p=1e-04), NIES981 (p=6e-04) and CZS25K (p=1e-04) in the 27 °C and 32 °C temperature groups, CZS48M (p=1e-04) was significantly associated with 17 °C, 22 °C, 27 °C groups, and CCMP836 (p=6e-04) was significantly associated with 22 °C, 27 °C, and 32 °C groups. Furthermore, a NMDS plot was made for both light and temperature levels to visualize centroid differences (Figure 9).

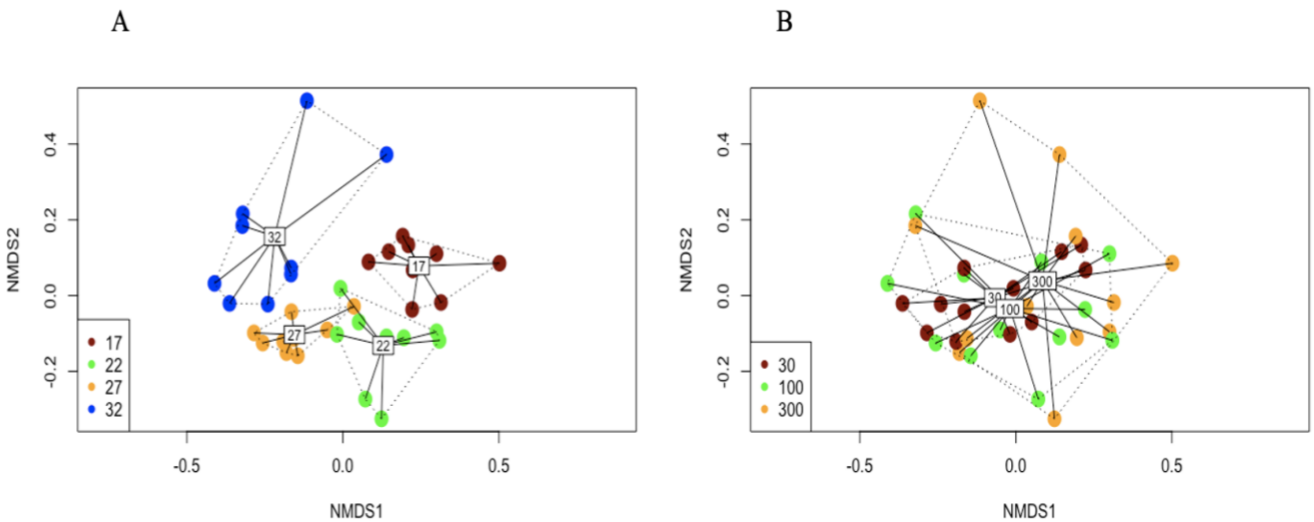

Figure 9: Non-metric multidimensional scaling (NMDS) plot showing temperature (A) and light (B) level Bray-Curtis distance visualizations for growth rate estimates of relative chlorophyll increases in six strains of picocyanobacteria. Light and temperature names indicate group centroids and dotted lines provide an estimate of group dispersion.

A two-way PERMANOVA was performed on the cell count growth rate estimate data as well, with a significant effect of temperature being detected ($F_{df=3}$ =6.76, p=0.0001), no significance of light ($F_{df=2}$ =0.58, p=0.76) and no significant interaction ($F_{df=6}$ =0.65, p=0.84). However, when we ran a multivariate homogeneity of variance test using the "betadisper" function from the "vegan" package to assess whether the significant PERMANOVA results were due to high variation in dispersion for both light and temperature levels, a significant result emerged (p=0.0020) for temperature, indicating that significance was likely due to high dispersion and not due to significant differences between centroids. This result is confirmed visually using an NMDS visualization of both light and temperature groups (Figure 10).

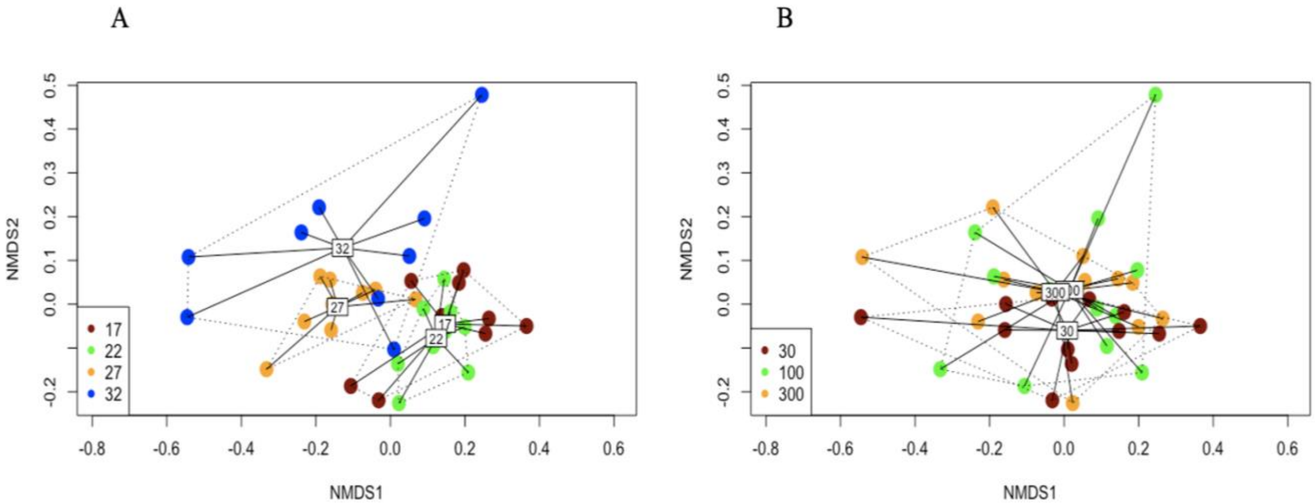

Figure 10: Non-metric multidimensional scaling (NMDS) plot showing temperature (A) and light (B) level Bray-Curtis distance visualizations for cell count growth rate estimates of six strains of picocyanobacteria. Light and temperature names indicate group centroids and dotted lines provide an estimate of group dispersion.

Due to the high degree of overlap on the temperature centroid distributions in the visualization in figure 10A we can suggest that no significant effect of temperature was found for this PERMANOVA analysis.

Strain Growth Optima Determination

To assess picocyanobacterial strain growth dynamics generalized additive modeling (GAM) was used. GAM models were constructed predicting growth rates for CCMP836, CCMP1333, CZS48M, NIES981, CZS25K, and PCC6803 across light and temperature levels (smoothing terms) using the “mgcv” package in RStudio. GAM values beyond >10% standard error were filtered out from the analysis. Furthermore, GAM results display top 10% percentile of growth rates per strain (Figure 11 & 12).

GAM modelling of chlorophyll content growth rates across environmental variables shows a diversity of strain responses (figure 11). PCC6803 shows a clear preference for high temperature conditions (>30 °C) and a wide tolerance for light levels. CCMP836 has a broad temperature distribution showing a preference for higher temperatures (>25 °C) and an aptitude for low light conditions. CZS25K also prefers high temperature conditions with a wide tolerance of light levels. CZS48M shows a preference at values around a 25 °C temperature level, and a relatively broad light level tolerance. NIES981 has a preference for low light conditions with the fastest chlorophyll increases being found at temperatures above 25 °C. CCMP1333 has a preference for mid-range light levels and a higher chlorophyll increases at high temperatures.

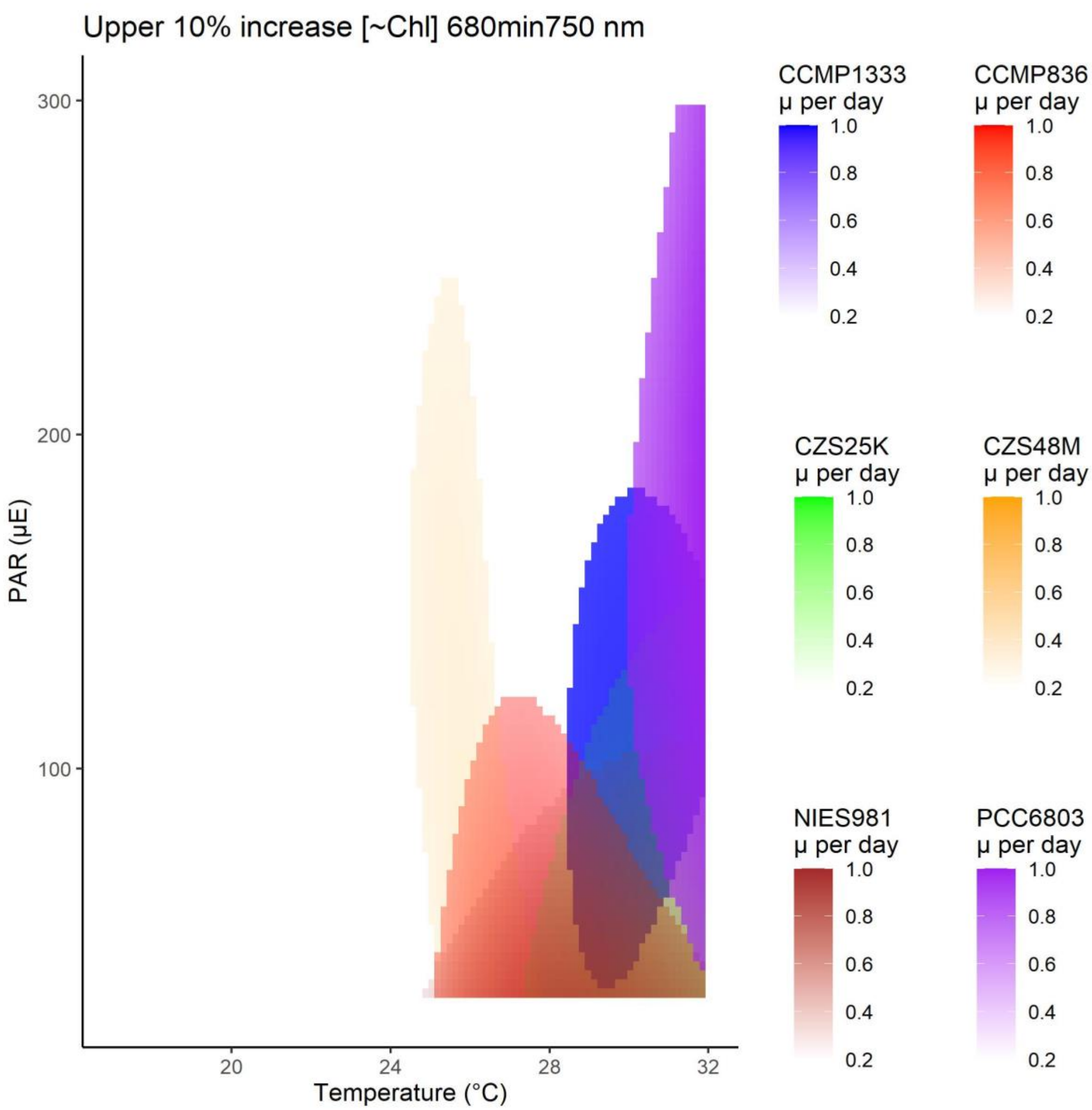

Figure 11: Visualization of the top 10% highest chlorophyll growth rates across a matrix of light and temperature conditions as predicted by generalized additive models for six strains of picocyanobacteria. Daily OD680-750 nm absorbance measurements (chlorophyll proxy) were made for each strain in all combinations of four temperature levels and three light levels, with these data being run in a regression against chlorophyll extractions at each condition tested. The resultant slope equation was used to calculate chlorophyll estimates which were then run through a modified Gompertz model which provided chlorophyll growth rates which were used for creating generalized additive models outlining optimal growth conditions.

Cell count growth rates were also used in GAM analysis to understand strain cell growth across environmental conditions (figure 12). PCC6803 can be seen to have a broad light aptitude and a preference for high temperature conditions. CCMP836 can be seen to grow fastest at lower light levels and at higher temperatures. CZS25K has a high temperature aptitude and grows fastest at all light levels above 100 µE. CZS48M grows fastest above 25 °C and at light levels above 100 µE. NIES981 can be seen to have its optimum temperature level just below 20 °C and its light preference is approximately 100-220 µE. CCMP 1333 also has a preference for light levels above and slightly below 100 µE and a preference for higher temperatures.

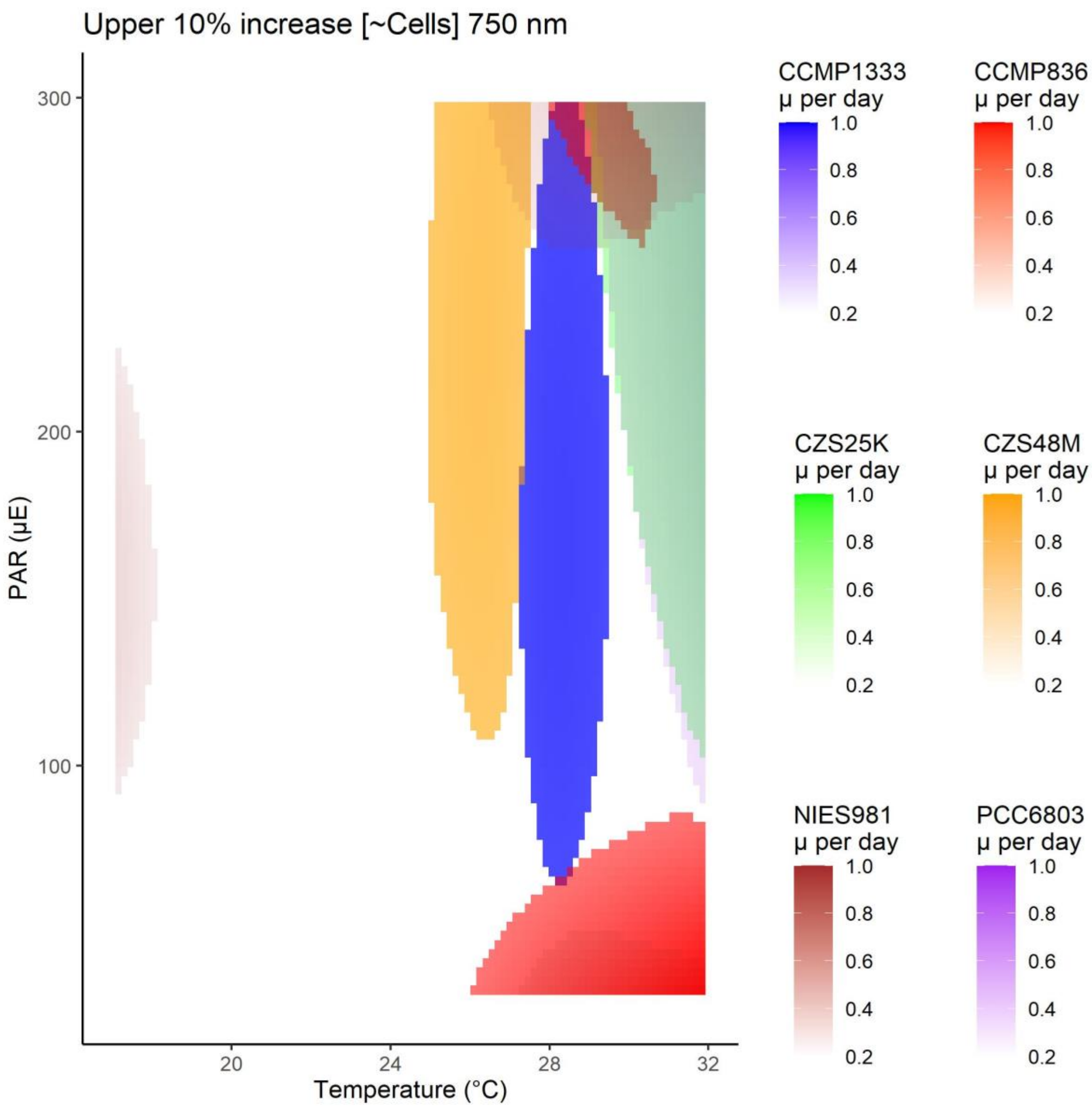

Figure 12: Visualization of the top 10% highest cell growth rates across a matrix of light and temperature conditions as predicted by generalized additive models for six strains of picocyanobacteria. Daily OD750 nm absorbance measurements (cell count proxy) were made for each strain in all combinations of four temperature levels and three light levels, with these data being run in a regression against cell counts at each condition tested. The resultant slope equation was used to calculate cell counts estimates which were then run through a modified Gompertz model which provided growth rates which were used for creating generalized additive models outlining optimal growth conditions.

Biovolume trends

Biovolume was measured for six strains of picocyanobacteria across three temperature levels and three light levels (Figure 13).

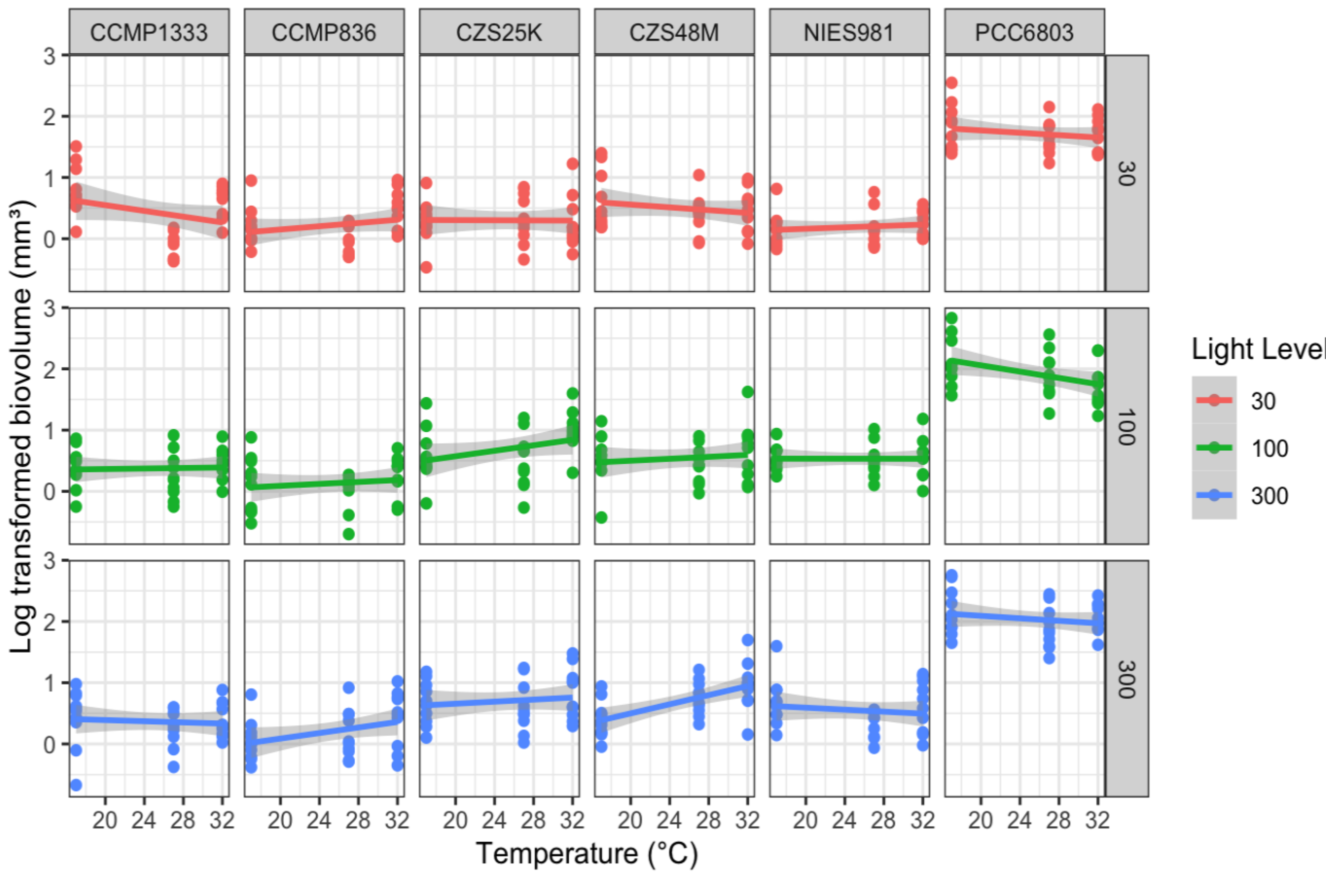

Figure 13: Biovolume measurements for six strains of picocyanobacteria across three light levels (µE) and three temperature levels. Biovolume measurements were performed ten times for each combination of light and temperature level by measuring length and width of cells. Resultant biovolume data were log transformed to keep strains comparable in their cell volume trends. No cell volume data is available for 22 °C data as culture pictures were not performed during trials at this temperature level

CCMP1333 displayed little difference in biovolume across temperature levels at 100 and 300 µE but experienced a decline in biovolume at 30 µE from 17 to 27 °C, with a brief increase in biovolume at 32 °C. CCMP836 experienced a gradual increase in biovolume with temperature at 30 µE with a brief dip at 27 °C, a relatively stable biovolume at 100 µE, and a gradual increase in biovolume with temperature at 300 µE. CZS25K experienced a stable biovolume across temperatures at 30 µE, a steady increase of biovolume with temperature at 100 µE, and a slight increase in biovolume at 300 µE. CZS48M can be seen to decrease slightly as temperatures rise at 30 µE, remain stable at 100 µE, and increase in biovolume as temperatures rise at 300 µE. NIES981 seems to be relatively stable in its biovolume across temperature levels at 30 and 100 µE, with a gradual decrease in biovolume at 300 µE. PCC6803 was shown to consistently decrease in its biovolume as temperature increased for all light levels.

Discussion

Potential mechanisms of temperature acclimation

Both marine and non-marine picocyanobacteria are a highly diverse group of organisms (Farrant *et al.* 2016, Callieri *et al.* 2013). This genetic diversity has allowed these organisms to succeed in a wide variety of temperature niches. As Farrant *et al.* (2016) demonstrated, distinct clades of picocyanobacteria that inhabit the same oceanic regions are genetically suited to their particular thermal environment, which suggests that broad picocyanobacterial distribution is in part generated by distinct genetic profiles which succeed in specialized thermal niche spaces. An example of this can be seen in the genera *Synechococcus*, as specific clades have been shown to be suited to specific thermal profiles which map on to their bio-geographical and latitudinal distributions (Zwirglmaier *et al.* 2008). A study performed by Pittera *et al.* (2014) found that distinct latitudinal thermal niches in *Synechococcus* could be linked to photosystem II (PSII) resilience to temperature gradients. This role of PSII resilience in picocyanobacterial thermotype distribution was further investigated by Pittera, Partensky, and Six (2017), who found that PSII resilience to temperature is dictated primarily through the temperature resilience of the phycocyanin rod component of the phycobilisome. This finding led Pittera, Partensky, and Six (2017) to hypothesize that during the colonization of colder climates phycobiliprotein molecular flexibility was selected over the thermal stability of the light harvesting complex. This finding suggests that one determinant factor in the latitudinal mobility of picocyanobacterial strains is the resilience of their light harvesting complexes to changes in temperature. Membrane thermostability has also been hypothesized to be an integral part of picocyanobacterial thermophysiology, as the regulation of membrane fluidity in response to changing temperature conditions is needed to maintain metabolic function (Mikami and Murata 2003). Pittera *et al.* (2018) found that specific thermotypes of picocyanobacteria expressed distinct desaturase enzymes, indicating that membrane regulation is an important factor in temperature niche adaptation. Given this information, we can hypothesize that differences in temperature growth optima may be due to variable thermostability of phycobilisome proteins and membrane fluidity regulation across picocyanobacterial strains. This would suggest that the strains used in this study all possess competent thermal membrane regulation and have been selected for PSII thermostability as opposed to membrane flexibility. To confirm this finding future studies may employ an analysis of phycobiliprotein denaturation curves and two-dimensional thin layer chromatography of picocyanobacterial lipid membranes.

Biovolume

Changes in temperature conditions have also been noted to induce physiological changes in cyanobacteria. Within this study, one notable physiological parameter that was observed to vary in response to temperature and light levels was biovolume (average cell dimensions). Broadly speaking, protists and bacteria tend to obey the "temperature-size rule" along thermal gradients, where average cell size decreases in increased temperature environments (Atkinson, Ciotti, and Montagnes 2003). While this trend has been observed in picocyanobacteria (Morán *et al.* 2010), it is not a consistent response across strains (Fu *et al.* 2007). Atkinson, Ciotti, and Montagnes (2003) hypothesized that the negative relationship between cell size and temperature could be a form of phenotypic plasticity which aims to slow sinking rates (as per Stokes equation), or to increase nutrient uptake efficiency due to smaller surface area to volume ratios. Another explanation provided by Atkinson, Ciotti, and Montagnes (2003) suggests that in an evolutionary context early reproduction is advantageous when population growth rates increase, as being able to exploit resources before the next generation of progeny would increase fitness. To facilitate early reproduction, cells would need to divide earlier, which would contribute to a lower average cell size in high temperature environments. Explanations for increases in cell sizes with increased temperatures are not well characterized in the literature, however one potential hypothesis lays in elemental quotas and resource availability. Fu *et al.* (2007) found that elemental quotas for *Prochlorococcus* strains doubled with increasing temperature, with Martiny *et al.* (2016) noting that increases in elemental quotas are associated with increases in cell size. These findings, along with the hypothesis proposed by Atkinson, Ciotti, and Montagnes (2003) stating that a positive temperature-cell size relationships may be found in increased temperature environments with no resource limitation, suggests that strains increasing in biovolume with temperature may do so as they require higher elemental quotas, and that their culture environments are not resource limited. Therefore, variable responses in biovolume with increases in temperature may indicate a diversity in nutrient requirements and growth optimization strategies across picocyanobacterial strains. This may suggest that strains NIES981, CCMP1333, and PCC6803 follow a phenotypic response to increasing temperature which aims to slow sinking and allow for more efficient nutrient uptake and reproduction, whereas strains CZS25K, CCMP836, and CZS48M follow a response which allows them to fulfill increasing nutrient quotas.

Light

Our statistical analyses on chlorophyll growth rates found a significant effect of light and temperature for all strains except for CCMP1333, with both CZS48M and CCMP836 exhibiting an interactive effect of these factors. The significance of light on pigment content in algal cells is well documented in the literature, as increased pigment expression at lower light levels and decreased pigment content at higher light levels is an established effect (Seyfabadi, Ramezanpour, and Amini Khoeyi 2011). Given that chlorophyll *a* is involved in light capture, it makes sense theoretically that it would be up-regulated in light limiting environments. This can be seen as a general explanation for why, across picophytoplankton, higher light levels yielded lower chlorophyll growth rates. This trend can be seen in figure 12, however certain strains do not follow this pattern such as PCC6803 whose chlorophyll growth rates were consistent for all light levels. We also found that temperature had a significant effect on chlorophyll growth rates both strain specifically and when picocyanobacterial strains as a whole were compared across temperature levels (figure 9). Lower chlorophyll *a* growth rates at lower temperatures could be attributed to a metabolic trade off, as polar cyanobacteria have been postulated to reduce chlorophyll *a* expression in sub-optimal temperature environments in order to increase rubisco production, which is limited in non-ideal thermal environments (Tang and Vincent 1999). Increased pigment contents have been noted at higher temperatures with some algal strains, as noted by Davison (1991), as perhaps the increased metabolic rate associated with higher temperatures (Dell, Pawar, and Savage 2011) necessitates more efficient light absorption. Interactive effects of temperature and light have also been noted in algal strains (Nicklisch, Shatwell, and Köhler 2008, X. Li *et al.* 2021). X. Li *et al.* (2021) found that temperature interacts with light to cause differences in photoinhibition, where increases in temperature were found to prevent photoinhibition. Although the opposite effect is detected for CSZ48M and CCMP836, a similar mechanistic relationship could be occurring. Furthermore, it was found that light, broadly speaking, had little effect of cell count growth rates. This finding would suggest a strong photo-acclimation capacity within picocyanobacterial strains within nutrient replete conditions.

Ecological Significance

We have detected that strain specific cell count growth rates are highly affected by temperature, with GAM modelling revealing that most strains find their cell count and chlorophyll growth rate optima at temperatures greater than 25 °C. Thus, given increases in water temperatures as a result of global warming, population scale changes may occur in the latitudinal distribution of picocyanobacteria. This conjecture is corroborated by Flombaum *et al.* (2013), who found that picocyanobacterial distribution was predominantly indicated by temperature. Furthermore, Flombaum *et al.* (2013) have predicted a 14% increase in *Synechococcus* abundance due to rising sea surface temperatures, and that this increase in abundance was associated with marginal latitudinal distribution expansions of tropical *Synechococcus*. The picocyanobacterial strains used in this study originate from a diverse phylogenetic and geographic distribution, with all strains originating from the same subclade, apart from PCC6803 which is an established model organism. Therefore, I performed an origin specific temperature trend investigation to predict the future growth trends of these strains in their respective habitats.

NIES981 is a picocyanobacterial strain isolated from coastal Okinawa (Yamaguchi *et al.*, 2016). Average water temperatures in this region rise to 29 °C in the summer, with a mean annual temperature of 26.41 °C (Japan Meteorological Agency, 2022). Since 1930 water temperatures near Okinawa have increased by 1.4 °C, with a 0.23 °C increase in temperature being predicted per decade (Hoegh-Guldberg, 2000). Cell count growth rates indicate that 17, 27, and 32 °C are the temperature growth optima for this strain. Given that there was no significant difference between the 27 and 32 °C temperature levels, we can predict that no significant shift in NIES981 cell count growth rates will occur with rising temperatures in the coming century. It is important to note, however, that the specific growth preferences for this strain are highly unusual as it does not show a typical growth response, as it shows high growth in high and low temperature environments, with low growth occurring in average temperatures. This bizarre response may be explained by culture contamination. CCMP836 was isolated from the coast of Tabasco in the Gulf of Mexico (Pichard and Campbell, 1997), which has a mean annual temperature of approximately 26-27 °C (NCEI, 2020), and can be estimated to increase by 0.20 °C per decade (Kibler *et al.* 2015), which would put the average temperature at approximately 28.1 °C by the end of the century. As seen in figure 7, as temperatures increase CCMP836 cell count growth preference shifts to lower light conditions. This may indicate that as temperatures rise this strain will occupy a niche space lower in the euphotic zone. CCMP1333 was isolated from the Long Island Sound (Taylor, Gobler, and Sañudo-Wilhelmy 2006) which experiences temperatures near 25 °C in the summer (US Department of Commerce, 2022). CCMP1333 showed growth optima at 27 °C for cell count growth rates. The Long Island Sound has been found to be warming 4 times faster than the global ocean estimates, with an estimated increase of 0.45 °C per decade (Snyder *et al.* 2019), which would put summer water temperatures peaking around 28.6 °C by the end of the century. This would place CCMP1333 within its optimal growth conditions, which would produce a ≈20% increase in growth based on the increase of cell count growth rates with temperature seen in figure 5. Both CZS48M and CZS25K were isolated from the Zingster Strom, where peak temperatures range from 20-22 °C (COPERNICUS-EU, 2022). Reports indicate a roughly 0.5 °C increase in temperature per decade across the entire Baltic sea (Stramska and Białogrodzka 2015). This would suggest a maximum temperature of approximately 25-26 °C at the end of this century. Cell count growth rates for CZS25K indicate a growth optima of 27-32 °C. Thus, based on cell count growth rate data seen in figure 4, we can expect a ≈18% increase in growth of CZS25K in the next 80 years. CZS48M displayed a similar cell count growth rate optima as CZS25K, as optimal growth was seen at 27 °C. This optimum, as seen in figure 8, would suggest a 44% increase in cell growth by the year 2100. PCC6803 was isolated from a freshwater lake in California (Ikeuchi and Tabata 2001). Peak temperatures found at lake Tahoe, the largest freshwater lake in California, were seen to be around 24 °C (U.S. Climate Data, 2022). A study performed by Schneider *et al.* (2009) found that on average, lakes found in the California and Nevada region are increasing in temperature by 1.1 °C per decade. This would indicate that by the year 2100 average peak lake water temperatures would be approximately 32 °C. Given that PCC6803 cell count growth optima is found at 32 °C (figure 3), this increase in temperature would result in a 40% increase in cell growth.

This predicted increase in picocyanobacterial growth over the next century may cause significant damage to global biogeochemical cycles and food webs. Algal overgrowth, in the form of algal blooms, can block access of sunlight to photosynthetic organisms at the bottom of water systems (Okey *et al.* 2004). As a result, hypoxic conditions can emerge and macrobenthos can perish which can lead to shifts in the nutrient cycling of water systems (Berthold and Campbell 2021). These shifts in nutrient cycling can take years to recover (Chorus *et al.* 2020), and consist of the release of phosphorous and iron from sediments and a corresponding decrease in nitrogen, both of which help create a positive feedback loop of phytoplankton growth. In addition to causing long lasting damage to biogeochemical cycles, excessive picocyanobacterial growth can cause significant damage to food webs. This is due to the fact that as picocyanobacteria outperform their competitors in warmer conditions (such as dinoflagellates and diatoms) the overall quality of the trophic system declines (Schmidt *et al.* 2020). This is because picocyanobacteria lack the nutritional benefits, such as their lack of omega-3 fatty acids (Jónasdóttir 2019), that are needed to contribute to healthy fish and copepod growth, development, and reproduction (Schmidt *et al.* 2020). If picocyanobacteria come to dominate water systems due to increasing temperatures, this can lead to food webs lacking their required nutritional content, which may negatively effect local and global food webs.

Conclusion

In conclusion, we have found that a general increase of the growth rates of picocyanobacterial communities can be anticipated within the next century. This increase in cell count growth rates, along with a strong aptitude for photo-acclimation, would suggest that massive overgrowth could occur in the coming years. This overgrowth could have devastating impacts on biogeochemical cycles and food webs. Therefore, more analysis should be taken to build better models that incorporate nutrient, photoperiod, and allelopathic data to help assess the threat of picocyanobacterial overgrowth in order for preventative and restorative measures to be taken.

Bibliography

Abonyi, András, Keve Tihamér Kiss, András Hidas, Gábor Borics, Gábor Várbíró, and Éva Ács. 2020. “Cell Size Decrease and Altered Size Structure of Phytoplankton Constrain Ecosystem Functioning in the Middle Danube River Over Multiple Decades.” *Ecosystems* 23 (6): 1254–64. *https://doi.org/10.1007/s10021-019-00467-6*.

Andersen, R.A. (2005) Algal Culturing Techniques, Elsevier.

Atkinson, David, Benjamin J Ciotti, and David J S Montagnes. 2003. “Protists Decrease in Size Linearly with Temperature: Ca. 2.5% Degrees C(-1).” *Proceedings of the Royal Society B: Biological Sciences* 270 (1533): 2605–11. *https://doi.org/10.1098/rspb.2003.2538*.

Banse, Karl. 1976. “Rates of Growth, Respiration and Photosynthesis of Unicellular Algae as Related to Cell Sizea Review1,2.” *Journal of Phycology* 12 (2): 135–40. *https://doi.org/10.1111/j.1529-8817.1976.tb00490.x*.

Baty F, Delignette-Muller M (2014). *nlsMicrobio: data sets and nonlinear regression models dedicated to predictive microbiology*. R package version 0.0-1.

Baty F, Ritz C, Charles S, Brutsche M, Flandrois J, Delignette-Muller M (2015). “A Toolbox for Nonlinear Regression in R: The Package nlstools.” *Journal of Statistical Software*, **66**(5), 1–21. doi: *10.18637/jss.v066.i05*, *https://www.jstatsoft.org/article/view/v066i05*.

Berges, John A., Daniel J. Franklin, and Paul J. Harrison. 2001. “Evolution of an Artificial Seawater Medium: Improvements in Enriched Seawater, Artificial Water Over the Last Two Decades.” *Journal of Phycology* 37 (6): 1138–45. *https://doi.org/10.1046/j.1529-8817.2001.01052.x*.

Berthold, Maximilian, and Douglas A Campbell. 2021. “Restoration, Conservation and Phytoplankton Hysteresis.” *Conservation Physiology* 9 (1). *https://doi.org/10.1093/conphys/coab062*.

Bibby, Thomas S., I. Mary, J. Nield, F. Partensky, and J. Barber. 2003. “Low-Light-Adapted Prochlorococcus Species Possess Specific Antennae for Each Photosystem.” *Nature* 424 (6952): 1051–54. *https://doi.org/10.1038/nature01933*.

Boehrer, Bertram, and Martin Schultze. 2008. “Stratification of Lakes.” *Reviews of Geophysics* 46 (2). *https://doi.org/10.1029/2006RG000210*.

Cabello-Yeves, Pedro J., Antonio Picazo, Antonio Camacho, Cristiana Callieri, Riccardo Rosselli, Juan J. Roda-Garcia, Felipe H. Coutinho, and Francisco Rodriguez-Valera. 2018. “Ecological and Genomic Features of Two Widespread Freshwater Picocyanobacteria.” *Environmental Microbiology* 20 (10): 3757–71. *https://doi.org/10.1111/1462-2920.14377*.

Callieri, Cristiana, Manuela Coci, Gianluca Corno, Miroslav Macek, Beatriz Modenutti, Esteban Balseiro, and Roberto Bertoni. 2013. “Phylogenetic Diversity of Nonmarine Picocyanobacteria.” *FEMS Microbiology Ecology* 85 (2): 293–301. *https://doi.org/10.1111/1574-6941.12118*.

Chorus, Ingrid, Antje Köhler, Camilla Beulker, Jutta Fastner, Klaus van de Weyer, Tilo Hegewald, and Michael Hupfer. 2020. “Decades Needed for Ecosystem Components to Respond to a Sharp and Drastic Phosphorus Load Reduction.” *Hydrobiologia* 847 (21): 4621–51. *https://doi.org/10.1007/s10750-020-04450-4*.

Clarke, A., and K. P. P. Fraser. 2004. “Why Does Metabolism Scale with Temperature?” *Functional Ecology* 18 (2): 243–51. *https://doi.org/10.1111/j.0269-8463.2004.00841.x*.

“Coastal Ecosystem Maps - Gulf of Mexico.” 2020. *National Centers for Environmental Information (NCEI)*. http://www.ncei.noaa.gov/products/coastal-ecosystem-maps-gulf-mexico.

Davison, Ian R. 1991. “Environmental Effects on Algal Photosynthesis: Temperature.” *Journal of Phycology* 27 (1): 2–8. *https://doi.org/10.1111/j.0022-3646.1991.00002.x*.

Dell, Anthony I., Samraat Pawar, and Van M. Savage. 2011. “Systematic Variation in the Temperature Dependence of Physiological and Ecological Traits.” *Proceedings of the National Academy of Sciences* 108 (26): 10591–96. *https://doi.org/10.1073/pnas.1015178108*.

Elzhov, T.V., Mullen, K.M., Spiess, A.-N., and Bolker, B. (2022) minpack.lm: R Interface to the Levenberg-Marquardt Nonlinear Least-Squares Algorithm Found in MINPACK, Plus Support for Bounds.

Farrant, Gregory K., Hugo Doré, Francisco M. Cornejo-Castillo, Frédéric Partensky, Morgane Ratin, Martin Ostrowski, Frances D. Pitt, *et al.* 2016. “Delineating Ecologically Significant

Taxonomic Units from Global Patterns of Marine Picocyanobacteria." *Proceedings of the National Academy of Sciences* 113 (24): E3365–74. *https://doi.org/10.1073/pnas.1524865113*.

Finkel, Zoe V., John Beardall, Kevin J. Flynn, Antonietta Quigg, T. Alwyn V. Rees, and John A. Raven. 2010. "Phytoplankton in a Changing World: Cell Size and Elemental Stoichiometry." *Journal of Plankton Research* 32 (1): 119–37. *https://doi.org/10.1093/plankt/fbp098*.

Flombaum, Pedro, José L. Gallegos, Rodolfo A. Gordillo, José Rincón, Lina L. Zabala, Nianzhi Jiao, David M. Karl, *et al.* 2013. "Present and Future Global Distributions of the Marine Cyanobacteria Prochlorococcus and Synechococcus." *Proceedings of the National Academy of Sciences* 110 (24): 9824–29. *https://doi.org/10.1073/pnas.1307701110*.

Fu, Fei-Xue, Mark E. Warner, Yaohong Zhang, Yuanyuan Feng, and David A. Hutchins. 2007. "Effects of Increased Temperature and Co2 on Photosynthesis, Growth, and Elemental Ratios in Marine Synechococcus and Prochlorococcus (Cyanobacteria)1." *Journal of Phycology* 43 (3): 485–96. *https://doi.org/10.1111/j.1529-8817.2007.00355.x*.

Gardner, Janet L., Anne Peters, Michael R. Kearney, Leo Joseph, and Robert Heinsohn. 2011. "Declining Body Size: A Third Universal Response to Warming?" *Trends in Ecology & Evolution* 26 (6): 285–91. *https://doi.org/10.1016/j.tree.2011.03.005*.

Harrison, Paul J., Rosemary E. Waters, and F. J. R. Taylor. 1980. "A Broad Spectrum Artificial Sea Water Medium for Coastal and Open Ocean Phytoplankton1." *Journal of Phycology* 16 (1): 28–35. *https://doi.org/10.1111/j.0022-3646.1980.00028.x*.

Hoegh-Guldberg, O. 2000. "Global Climate Change and the Thermal Tolerance of Corals." Journal of the Japanese Coral Reef Society, 2000 (2): 1–11. *https://doi.org/10.3755/jcrs.2000.1*.

Ikeuchi, Masahiko, and Satoshi Tabata. 2001. "Synechocystis Sp. PCC 6803 a Useful Tool in the Study of the Genetics of Cyanobacteria." *Photosynthesis Research* 70 (1): 73–83. *https://doi.org/10.1023/A:1013887908680*.

"Japan Meteorological Agency | Sea Surface Temperature (Around Japan)." Date accessed: April 2022, https://www.data.jma.go.jp/gmd/kaiyou/english/long_term_sst_japan/sea_surface_temperature_around_japan.html.

Jasser, Iwona, and Cristiana Callieri. 2016. “Picocyanobacteria.” In *Handbook of Cyanobacterial Monitoring and Cyanotoxin Analysis*, 19–27. John Wiley & Sons, Ltd. *https://doi.org/10.1002/9781119068761.ch3*.

Jónasdóttir, Sigrún Huld. 2019. “Fatty Acid Profiles and Production in Marine Phytoplankton.” *Marine Drugs* 17 (3): 151. *https://doi.org/10.3390/md17030151*.

Kibler, Steven R., Patricia A. Tester, Kenneth E. Kunkel, Stephanie K. Moore, and R. Wayne Litaker. 2015. “Effects of Ocean Warming on Growth and Distribution of Dinoflagellates Associated with Ciguatera Fish Poisoning in the Caribbean.” *Ecological Modelling* 316 (November): 194–210. *https://doi.org/10.1016/j.ecolmodel.2015.08.020*.

Kim, Yihwan, Jehyun Jeon, Min Seok Kwak, Gwang Hoon Kim, InSong Koh, and Mina Rho. 2018. “Photosynthetic Functions of Synechococcus in the Ocean Microbiomes of Diverse Salinity and Seasons.” *PLoS ONE* 13 (1): e0190266. *https://doi.org/10.1371/journal.pone.0190266*.

Komárek, Jiří, Jeffrey R. Johansen, Jan Šmarda, and Otakar Strunecký. 2020. “Phylogeny and Taxonomy of Synechococcus-like Cyanobacteria.” *Fottea* 20 (2): 171–91. *https://doi.org/10.5507/fot.2020.006*.

Komenda, Josef, Martin Tichý, Ondřej Prášil, Jana Knoppová, Stanislava Kuviková, Remco de Vries, and Peter J. Nixon. 2007. “The Exposed N-Terminal Tail of the D1 Subunit Is Required for Rapid D1 Degradation During Photosystem II Repair in Synechocystis Sp PCC 6803.” *The Plant Cell* 19 (9): 2839–54. *https://doi.org/10.1105/tpc.107.053868*.

Larsson, John, Narin Celepli, Karolina Ininbergs, Christopher L. Dupont, Shibu Yooseph, Bigitta Bergman, and Martin Ekman. 2014. “Picocyanobacteria Containing a Novel Pigment Gene Cluster Dominate the Brackish Water Baltic Sea.” *The ISME Journal* 8 (9): 1892–1903. *https://doi.org/10.1038/ismej.2014.35*.

Li, Guancheng, Lijing Cheng, Jiang Zhu, Kevin E. Trenberth, Michael E. Mann, and John P. Abraham. 2020. “Increasing Ocean Stratification over the Past Half-Century.” *Nature Climate Change* 10 (12): 1116–23. *https://doi.org/10.1038/s41558-020-00918-2*.

Li, Xiangpeng, Jacob Manuel, Shelyn Slavens, Daniel W. Crunkleton, and Tyler W. Johannes. 2021. “Interactive Effects of Light Quality and Culturing Temperature on Algal Cell Size, Biomass Doubling Time, Protein Content, and Carbohydrate Content.” *Applied Microbiology and Biotechnology* 105 (2): 587–97. *https://doi.org/10.1007/s00253-020-11068-y*.

Lopes, Viviana R., Vitor Ramos, António Martins, Marcos Sousa, Martin Welker, Agostinho Antunes, and Vítor M. Vasconcelos. 2012. “Phylogenetic, Chemical and Morphological Diversity of Cyanobacteria from Portuguese Temperate Estuaries.” *Marine Environmental Research* 73 (February): 7–16. *https://doi.org/10.1016/j.marenvres.2011.10.005*.

Martiny, Adam C., Lanying Ma, Céline Mouginot, Jeremy W. Chandler, and Erik R. Zinser. 2016. “Interactions Between Thermal Acclimation, Growth Rate, and Phylogeny Influence Prochlorococcus Elemental Stoichiometry.” *PLOS ONE* 11 (12): e0168291. *https://doi.org/10.1371/journal.pone.0168291*.

Mikami, Koji, and Norio Murata. 2003. “Membrane Fluidity and the Perception of Environmental Signals in Cyanobacteria and Plants.” *Progress in Lipid Research* 42 (6): 527–43. *https://doi.org/10.1016/S0163-7827(03)00036-5*.

Morán, Xosé Anxelu G., Ángel López-Urrutia, Alejandra Calvo-Díaz, and William K. W. Li. 2010. “Increasing Importance of Small Phytoplankton in a Warmer Ocean.” *Global Change Biology* 16 (3): 1137–44. *https://doi.org/10.1111/j.1365-2486.2009.01960.x*.

Mousing, Erik A., Sofia Ribeiro, Chelsea Chisholm, Antoon Kuijpers, Matthias Moros, and Marianne Ellegaard. 2017. “Size Differences of Arctic Marine Protists Between Two Climate Periodsusing the Paleoecological Record to Assess the Importance of Within-Species Trait Variation.” *Ecology and Evolution* 7 (1): 3–13. *https://doi.org/10.1002/ece3.2592*.

Mulo, Paula, Cosmin Sicora, and Eva-Mari Aro. 2009. “Cyanobacterial psbA Gene Family: Optimization of Oxygenic Photosynthesis.” *Cellular and Molecular Life Sciences* 66 (23): 3697–3710. *https://doi.org/10.1007/s00018-009-0103-6*.

Mundim, Kleber C., Solange Baraldi, Hugo G. Machado, and Fernando M. C. Vieira. 2020. "Temperature Coefficient (Q10) and Its Applications in Biological Systems: Beyond the Arrhenius Theory." *Ecological Modelling* 431 (September): 109127. *https://doi.org/10.1016/j.ecolmodel.2020.109127*.

Murphy, Cole D., Mitchell S. Roodvoets, Emily J. Austen, Allison Dolan, Audrey Barnett, and Douglas A. Campbell. 2017. "Photoinactivation of Photosystem II in Prochlorococcus and Synechococcus." *PLOS ONE* 12 (1): e0168991. *https://doi.org/10.1371/journal.pone.0168991*.

Naselli-Flores, Luigi, Tamar Zohary, and Judit Padisák. 2021. "Life in Suspension and Its Impact on Phytoplankton Morphology: An Homage to Colin S. Reynolds." *Hydrobiologia* 848 (1): 7–30. *https://doi.org/10.1007/s10750-020-04217-x*.

Nicklisch, Andreas, Tom Shatwell, and Jan Köhler. 2008. "Analysis and Modelling of the Interactive Effects of Temperature and Light on Phytoplankton Growth and Relevance for the Spring Bloom." *Journal of Plankton Research* 30 (1): 75–91. *https://doi.org/10.1093/plankt/fbm099*.

Oksanen, J., Blanchet, F.G., Kindt, R., Legendre, P., Minchin, P.R., O'hara, R.B., et al. (2013) Community ecology package. *R package version* **2**:.

Okey, Thomas A, Gabriel A Vargo, Steven Mackinson, Marcelo Vasconcellos, Behzad Mahmoudi, and Cynthia A Meyer. 2004. "Simulating Community Effects of Sea Floor Shading by Plankton Blooms over the West Florida Shelf." *Ecological Modelling*, Placing Fisheries in their Ecosystem Context, 172 (2): 339–59. *https://doi.org/10.1016/j.ecolmodel.2003.09.015*.

Partensky, F., W. R. Hess, and D. Vaulot. 1999. "Prochlorococcus, a Marine Photosynthetic Prokaryote of Global Significance." *Microbiology and Molecular Biology Reviews* 63 (1): 106–27.

Peleg, Micha, and Maria G. Corradini. 2011. "Microbial Growth Curves: What the Models Tell Us and What They Cannot." *Critical Reviews in Food Science and Nutrition* 51 (10): 917–45. *https://doi.org/10.1080/10408398.2011.570463*.

Pichard, S.L., Campbell, L., and Paul, J.H. (1997) Diversity of the ribulose bisphosphate carboxylase/oxygenase form I gene (rbcL) in natural phytoplankton communities. *Appl Environ Microbiol* **63**: 3600–3606.
Pittera, Justine, Florian Humily, Maxine Thorel, Daphné Grulois, Laurence Garczarek, and Christophe Six. 2014. "Connecting Thermal Physiology and Latitudinal Niche Partitioning in Marine Synechococcus." *The ISME Journal* 8 (6): 1221–36. *https://doi.org/10.1038/ismej.2013.228*.

Pittera, Justine, Juliette Jouhet, Solène Breton, Laurence Garczarek, Frédéric Partensky, Éric Maréchal, Ngoc A. Nguyen, *et al.* 2018. "Thermoacclimation and Genome Adaptation of the Membrane Lipidome in Marine Synechococcus." *Environmental Microbiology* 20 (2): 612–31. *https://doi.org/10.1111/1462-2920.13985*.

Pittera, Justine, Frédéric Partensky, and Christophe Six. 2017. "Adaptive Thermostability of Light-Harvesting Complexes in Marine Picocyanobacteria." *The ISME Journal* 11 (1): 112–24. *https://doi.org/10.1038/ismej.2016.102*.

Pulina, Silvia, Andreas Brutemark, Sanna Suikkanen, Bachisio M. Padedda, Lorena M. Grubisic, Cecilia T. Satta, Tiziana Caddeo, Pasqualina Farina, Nicola Sechi, and Antonella Lugliè. 2016. "Effects of Warming on a Mediterranean Phytoplankton Community." *Web Ecology* 16 (1): 89–92. *https://doi.org/10.5194/we-16-89-2016*.

Rosas-Navarro, Anaid, Gerald Langer, and Patrizia Ziveri. 2018. "Temperature Effects on Sinking Velocity of Different Emiliania Huxleyi Strains." *PLoS ONE* 13 (3): e0194386. *https://doi.org/10.1371/journal.pone.0194386*.

RStudio Team (2020). RStudio: Integrated Development for R. RStudio, PBC, Boston, MA URL http://www.rstudio.com/.

Salewski, Volker, and Cortney Watt. 2017. "Bergmann's Rule: A Biophysiological Rule Examined in Birds." *Oikos* 126 (2). *https://doi.org/10.1111/oik.03698*.

Scanlan, D., M. Ostrowski, S. Mazard, A. Dufresne, L. Garczarek, W. Hess, A. Post, M. Hagemann, I. Paulsen, and F. Partensky. 2009. "Ecological Genomics of Marine

Picocyanobacteria." *Microbiology and Molecular Biology Reviews*. *https://doi.org/10.1128/MMBR.00035-08*.

Schmidt, Katrin, Antony J. Birchill, Angus Atkinson, Robert J. W. Brewin, James R. Clark, Anna E. Hickman, David G. Johns, *et al.* 2020. "Increasing Picocyanobacteria Success in Shelf Waters Contributes to Long-Term Food Web Degradation." *Global Change Biology* 26 (10): 5574–87. *https://doi.org/10.1111/gcb.15161*.

Schneider, P., S. J. Hook, R. G. Radocinski, G. K. Corlett, G. C. Hulley, S. G. Schladow, and T. E. Steissberg. 2009. "Satellite Observations Indicate Rapid Warming Trend for Lakes in California and Nevada." *Geophysical Research Letters* 36 (22). *https://doi.org/10.1029/2009GL040846*.

Sciascia, R., S. De Monte, and A. Provenzale. 2013. "Physics of Sinking and Selection of Plankton Cell Size." *Physics Letters A* 377 (6): 467–72. *https://doi.org/10.1016/j.physleta.2012.12.020*.

COPERNICUS programme, European Union, "Sea Surface Temperature (SST TAC) | CMEMS." Accessed: April 2022, https://marine.copernicus.eu/about/producers/sst-tac.

Seyfabadi, Jafar, Zohreh Ramezanpour, and Zahra Amini Khoeyi. 2011. "Protein, Fatty Acid, and Pigment Content of Chlorella Vulgaris Under Different Light Regimes." *Journal of Applied Phycology* 23 (4): 721–26. *https://doi.org/10.1007/s10811-010-9569-8*.

Six, Christophe, Zoe V. Finkel, Andrew J. Irwin, and Douglas A. Campbell. 2007. "Light Variability Illuminates Niche-Partitioning Among Marine Picocyanobacteria." *PLOS ONE* 2 (12): e1341. *https://doi.org/10.1371/journal.pone.0001341*.

Snyder, Jacob T., Michael M. Whitney, Hans G. Dam, Molly W. Jacobs, and Hannes Baumann. 2019. "Citizen Science Observations Reveal Rapid, Multi-Decadal Ecosystem Changes in Eastern Long Island Sound." *Marine Environmental Research* 146 (April): 80–88. *https://doi.org/10.1016/j.marenvres.2019.03.007*.

Sommer, Ulrich, Kalista H. Peter, Savvas Genitsaris, and Maria Moustaka-Gouni. 2017. "Do Marine Phytoplankton Follow Bergmann's Rule Sensu Lato?" *Biological Reviews* 92 (2): 1011–26. *https://doi.org/10.1111/brv.12266*.

Stanier, Roger Y., Josette Deruelles, Rosmarie Rippka, Michael Herdman, and John B. Waterbury. 1979. "Generic Assignments, Strain Histories and Properties of Pure Cultures of Cyanobacteria." *Microbiology*, March. *https://doi.org/10.1099/00221287-111-1-1*.

Stockner, John G. 1988. "Phototrophic Picoplankton: An Overview from Marine and Freshwater Ecosystems." *Limnology and Oceanography* 33 (4part2): 765–75. *https://doi.org/10.4319/lo.1988.33.4part2.0765*.

Stomp, Maayke, Jef Huisman, Floris de Jongh, Annelies J. Veraart, Daan Gerla, Machteld Rijkeboer, Bas W. Ibelings, Ute I. A. Wollenzien, and Lucas J. Stal. 2004. "Adaptive Divergence in Pigment Composition Promotes Phytoplankton Biodiversity." *Nature* 432 (7013): 104–7. *https://doi.org/10.1038/nature03044*.

Stramska, Malgorzata, and Jagoda Białogrodzka. 2015. "Spatial and Temporal Variability of Sea Surface Temperature in the Baltic Sea Based on 32-Years (1982) of Satellite Data." *Oceanologia* 57 (3): 223–35. *https://doi.org/10.1016/j.oceano.2015.04.004*.

Tang, Evonne P. Y., and Warwick F. Vincent. 1999. "Strategies of Thermal Adaptation by High-Latitude Cyanobacteria." *The New Phytologist* 142 (2): 315–23.

Taylor, Gordon T., Christopher J. Gobler, and Sergio A. Sañudo-Wilhelmy. 2006. "Speciation and Concentrations of Dissolved Nitrogen as Determinants of Brown Tide Aureococcus Anophagefferens Bloom Initiation." *Marine Ecology Progress Series* 312 (April): 67–83. *https://doi.org/10.3354/meps312067*.

Thompson, Anne W., Ger van den Engh, Nathan A. Ahlgren, Kathleen Kouba, Samantha Ward, Samuel T. Wilson, and David M. Karl. 2018. "Dynamics of Prochlorococcus Diversity and Photoacclimation During Short-Term Shifts in Water Column Stratification at Station ALOHA." *Frontiers in Marine Science* 5: 488. *https://doi.org/10.3389/fmars.2018.00488*.

US Department of Commerce, National Oceanic and Atmospheric Administration. n.d. "NDBC Station Page." http://www.ndbc.noaa.gov/station_page.php?station=44039.

Van de Waal, Dedmer B., and Elena Litchman. 2020. "Multiple Global Change Stressor Effects on Phytoplankton Nutrient Acquisition in a Future Ocean." *Philosophical Transactions of the Royal Society B: Biological Sciences* 375 (1798): 20190706. *https://doi.org/10.1098/rstb.2019.0706*.

"Weather Averages South Lake Tahoe, California." Date accessed: April 2022, https://www.usclimatedata.com/climate/south-lake-tahoe/california/united-states/usca1317.

Winder, Monika, John E Reuter, and S. Geoffrey Schladow. 2009. "Lake Warming Favours Small-Sized Planktonic Diatom Species." *Proceedings of the Royal Society B: Biological Sciences* 276 (1656): 427–35. *https://doi.org/10.1098/rspb.2008.1200*.

Wickham, H., Averick, M., Bryan, J., Chang, W., McGowan, L.D., François, R., et al. (2019) Welcome to the Tidyverse. *Journal of Open Source Software* **4**: 1686.

Yamaguchi, Haruyo, Yohei Shimura, Shigekatsu Suzuki, Takahiro Yamagishi, Norihisa Tatarazako, and Masanobu Kawachi. 2016. "Complete Genome Sequence of Cyanobium Sp. NIES-981, a Marine Strain Potentially Useful for Ecotoxicological Bioassays." *Genome Announcements* 4 (4): e00736–16. *https://doi.org/10.1128/genomeA.00736-16*.

Yvon-Durocher, Gabriel, José M. Montoya, Mark Trimmer, and Guy Woodward. 2011. "Warming Alters the Size Spectrum and Shifts the Distribution of Biomass in Freshwater Ecosystems." *Global Change Biology* 17 (4): 1681–94. *https://doi.org/10.1111/j.1365-2486.2010.02321.x*.

Zandalinas, Sara I., Felix B. Fritschi, and Ron Mittler. 2021. "Global Warming, Climate Change, and Environmental Pollution: Recipe for a Multifactorial Stress Combination Disaster." *Trends in Plant Science*, Special issue: Feeding the World: The Future of Plant Breeding, 26 (6): 588–99. *https://doi.org/10.1016/j.tplants.2021.02.011*.

Zohary, Tamar, Tatiana Fishbein, Miriam Shlichter, and Luigi Naselli-Flores. 2017. “Larger Cell or Colony Size in Winter, Smaller in Summer a Pattern Shared by Many Species of Lake Kinneret Phytoplankton.” *Inland Waters* 7 (2): 200–209. *https://doi.org/10.1080/20442041.2017.1320505*.

Zohary, Tamar, Giovanna Flaim, and Ulrich Sommer. 2021. “Temperature and the Size of Freshwater Phytoplankton.” *Hydrobiologia* 848 (1): 143–55. *https://doi.org/10.1007/s10750-020-04246-6*.

Zwietering, M. h., Rombouts, F. m., and Riet, K. van ’t (1992) Comparison of definitions of the lag phase and the exponential phase in bacterial growth. *Journal of Applied Bacteriology* **72**: 139–145.

Zwirglmaier, Katrin, Ludwig Jardillier, Martin Ostrowski, Sophie Mazard, Laurence Garczarek, Daniel Vaulot, Fabrice Not, Ramon Massana, Osvaldo Ulloa, and Dave J. Scanlan. 2008. “Global Phylogeography of Marine Synechococcus and Prochlorococcus Reveals a Distinct Partitioning of Lineages Among Oceanic Biomes.” *Environmental Microbiology* 10 (1): 147–61. *https://doi.org/10.1111/j.1462-2920.2007.01440.x*.

Appendix

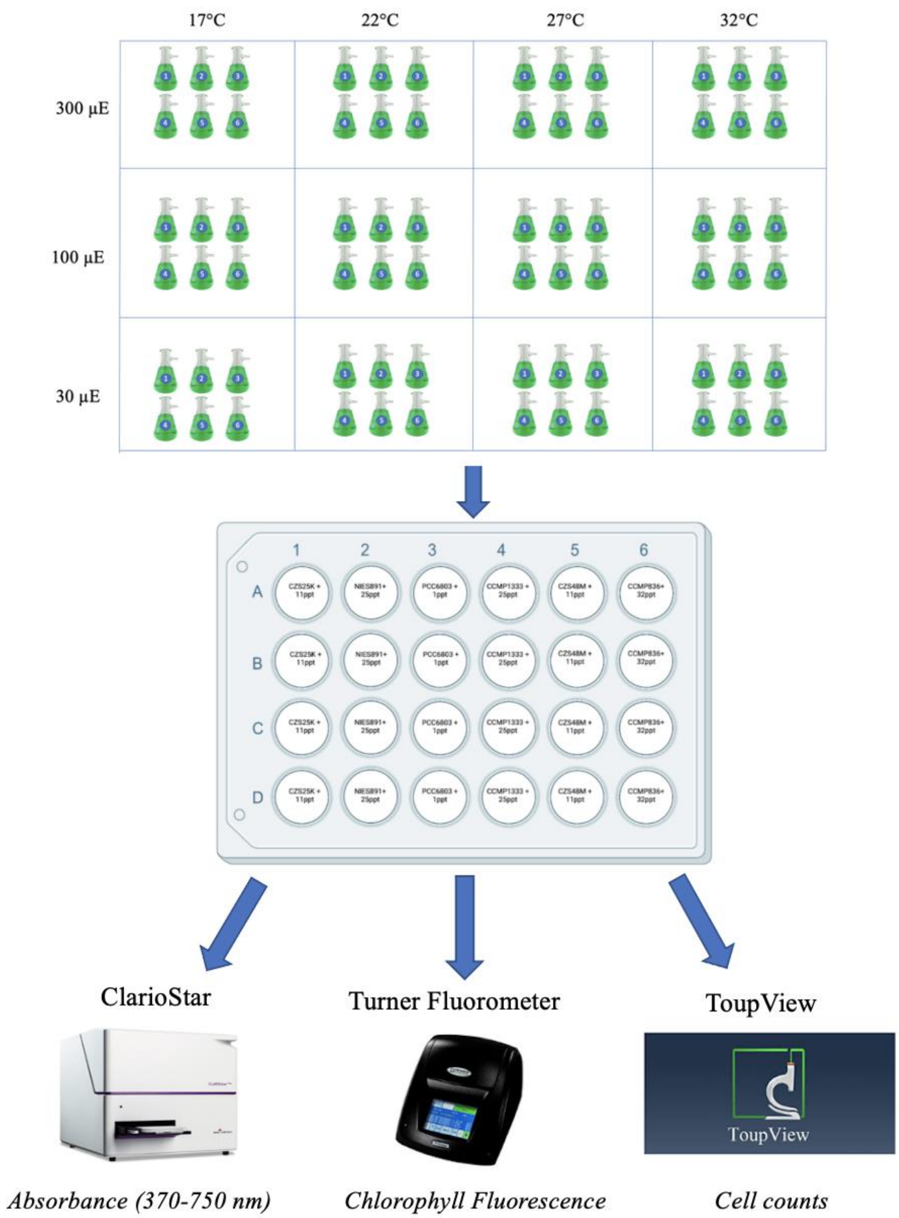

Figure 1: Schematic diagram outlining experimental protocol. Six strains of picocyanobacteria were grown in a matrix of conditions consisting of four temperature levels and three light levels using a well plate approach, where each strain was grown in its optimal salinity condition and was replicated four times within each plate. When cultures grown in these interacting conditions had undergone a doubling in their absorbance (deltaOD) as measured by the ClarioStar, chlorophyll extractions and cell counts were performed, using the Turner fluorometer and ToupView software respectively.

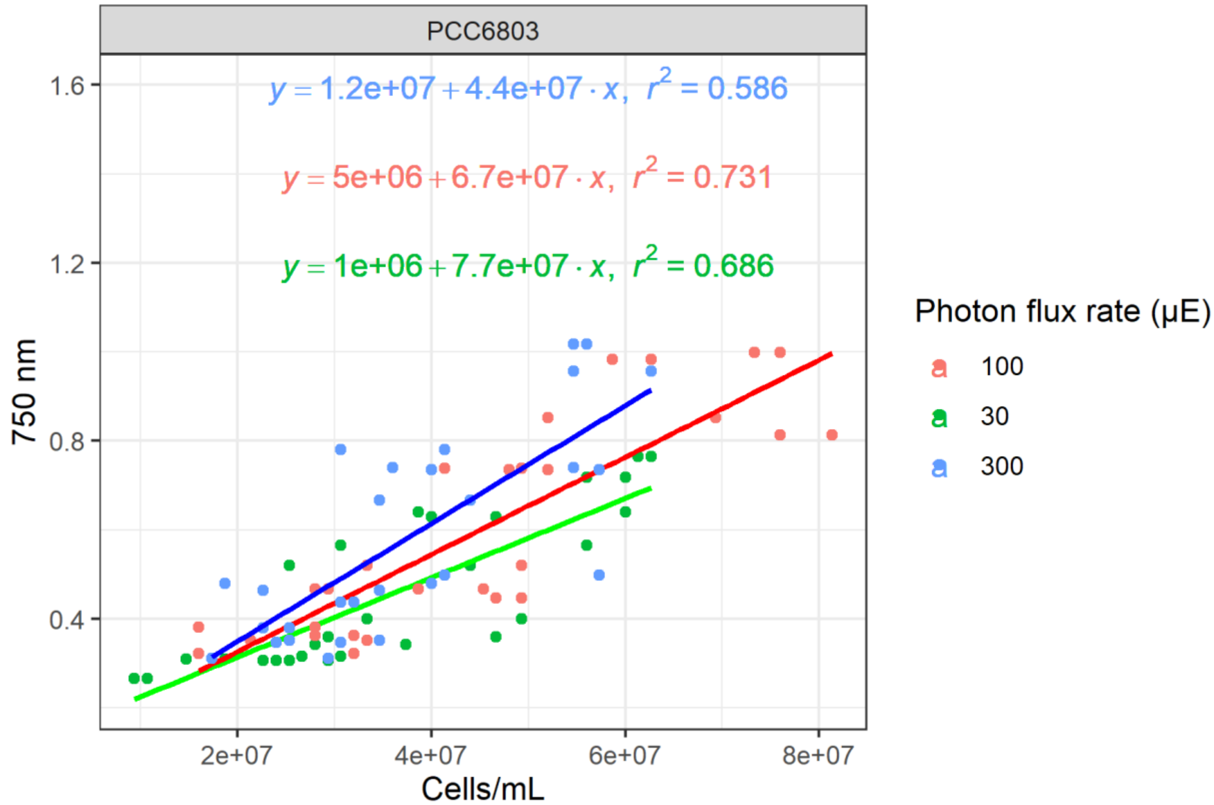

Figure 2: Regression performed between cell count data and OD750 nm absorbance measurements for PCC6803. Cell counts were performed whenever cultures had undergone a doubling in their optical density (deltaOD). The OD750 nm absorbance data provides a proxy for cell counts. This relationship between cell counts and OD750 nm was corrected using a regression between the absorbance measurements and their corresponding cell counts, which provides a slope equation which gives a mathematical relationship between OD750 nm values and cells per mL.

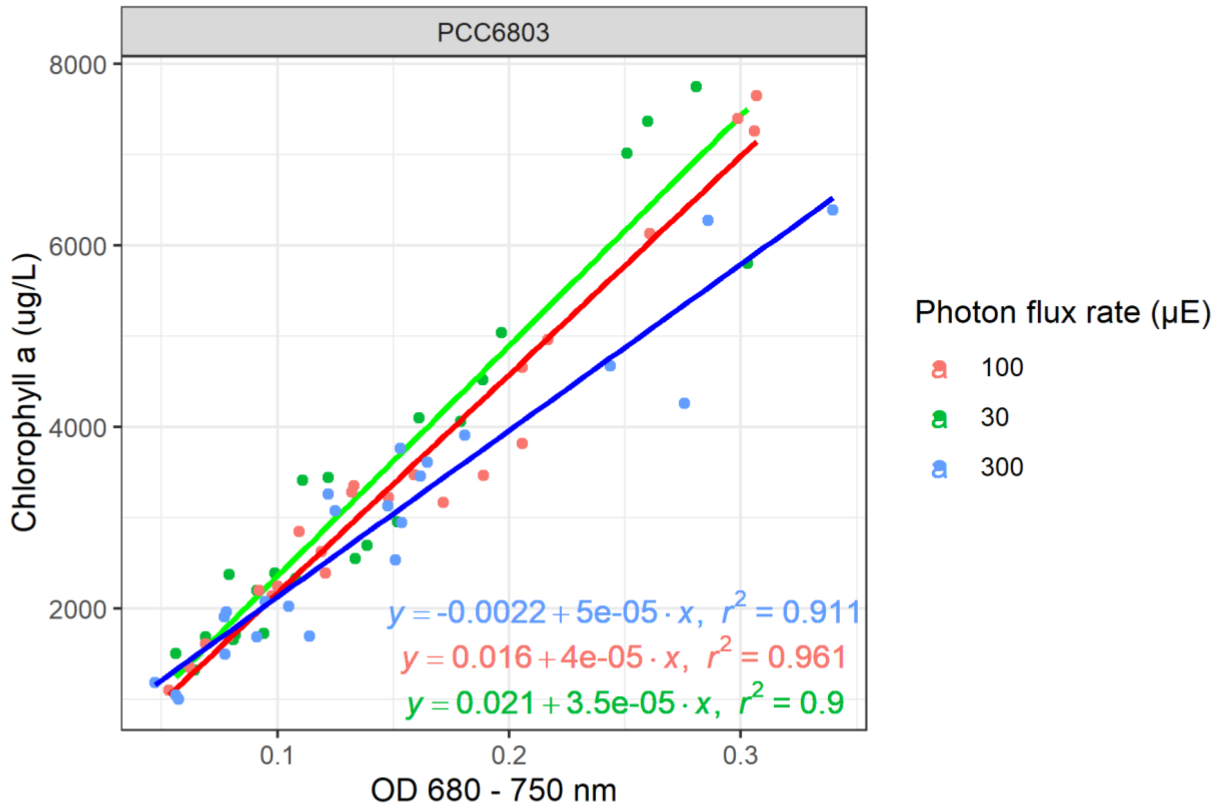

Figure 3: Regression performed between chlorophyll extraction data and deltaOD absorbance measurements for PCC6803. Chlorophyll extractions were performed whenever cultures had undergone a doubling in their optical density (deltaOD). The deltaOD absorbance data provides a proxy for chlorophyll content. This relationship between chlorophyll and deltaOD was corrected using a regression between the absorbance measurements and their corresponding chlorophyll extractions, which provides a slope equation which gives a mathematical relationship between deltaOD values and chlorophyll content in μg/L.